2017

Detecting Overpressure Zones by Using Model Based Inversion in Kupe Field, New Zealand

Timucin Cakir
Michigan Technological University, tcakir@mtu.edu

DETECTING OVERPRESSURE ZONES BY USING MODEL BASED INVERSION IN KUPE FIELD, NEW ZEALAND

By

Timucin Cakir

A THESIS

Submitted in partial fulfillment of the requirements for the degree of

MASTER OF SCIENCE

In Geophysics

MICHIGAN TECHNOLOGICAL UNIVERSITY

2017

This thesis has been approved in partial fulfillment of the requirements for the Degree of MASTER OF SCIENCE in Geophysics.

Department of Geological and Mining Engineering and Sciences

Thesis Advisor: *Dr. Wayne D. Pennington*

Committee Member: *Prof. Mir Sadri-Sabet*

Committee Member: *Assoc. Prof. Gregory P. Waite*

Department Chair: *Dr. John S. Gierke*

Table of Contents

List of Figures

List of Tables

Acknowledgements

I'd like to thank to my advisor, Prof. Wayne D. Pennington, who helped me to achieve my goals with his suggestions. His point of view has deepened my horizons on studying my thesis. His recommendations about choosing my thesis topic helped me to focus on my main topic, which is related to reservoir characterization.

I also would like to thank to committee members, Prof. Mir Sadri- Sabet and Assoc. Prof. Gregory P. Waite for their support and suggestions.

I am very grateful to Emre Doguturk for helping me to learn to use Hampson Russell Software.

I also appreciate to Fatma Sinem Boyaci for her contributions to my thesis with her valuable ideas.

Turkish Petroleum Company deserves the big acknowledgement for giving me a chance to study abroad. I'd like to thank to Hampson Russell Software to let me process my data and complete my thesis. Thanks to the New Zealand government and GNS Science to provide this dataset to me.

I am very happy that my family members Mehmet Cakir, Emine Cakir and Merve Burcin Cakir supported me during my research in Michigan Tech. They were always with me in my tough times.

Abstract

Overpressure is a significant parameter during a drilling process in oil exploration. This phenomenon happens when pore pressure exceeds the limit of hydrostatic pressure in a formation and causes drastic hazards such as blow outs while drilling. This thesis focuses on the determination of possible overpressure areas and studies at three wells in Kupe field, which is considered to be a natural-gas field in Taranaki Basin. In an effort to identify potential overpressure zones at the Kupe Field, acoustic impedance responses of 3D seismic data for three wells, along with their well log responses were evaluated.

Seismic inversion plays an important role in identifying overpressure zones. Thus, wavelet extraction, well correlation (well-tie), horizon determination and picking, then model-based seismic inversion, calibrating pressure to well logs and seismic data were applied to Kerry 3D post stack seismic data to obtain acoustic impedance and a pore pressure map, which are the important indicators of overpressure existence. With the findings of pore pressure values, we are able to predict and determine the location of overpressure zone in the Otaraoa Formation in Kupe Field. This analysis was supported by well log responses in the zone. Kupe South-1 well, Kupe South-2 well and Kupe-1 well log responses were evaluated besides their mud change parameters indicated overpressured zones. Density and sonic log responses were examined for each of three wells. The intervals of potential overpressure location determined by seismic acoustic impedance and a pore pressure that shows a reasonable consistency with well log and mud change data.

1. Introduction

Overpressure, which is the condition of greater pore pressure than hydrostatic pressure in a formation, has widely been encountered at the exploration wells in the Taranaki basin (Darby et al., 2000; Lowry, 2006; Webster and Adams, 1996; Shell Todd Oil Services Limited, 2002). Active tectonics, rapid deposition of sediments, horizontal stress and rapid generation of gas in low permeability are the reasons of overpressure in this basin (Webster et al., 2010). Overpressure may lead to dangerous situations during drilling, such as blowouts, thus overpressure zones should be determined and wells should be prepared to avoid drilling hazards.

Overpressure has been determined by using many approaches based on seismic measurement, conventional log analysis, and drilling event reports. This study mainly focuses on obtaining a pore pressure map to identify overpressure zones in the field. Seismic results are supported by well log analysis and drilling reports.

One of the mechanisms that overpressure is present is the loading mechanism. Compaction disequilibrium is a loading mechanism that is seen in Kupe Field (Webster et al., 2010). By knowing that compaction disequilibrium is a cause of overpressure, we try to identify the overpressured area in this field.

Additionally, mud change is another parameter that gives an idea about overpressure existence in a formation. Mud weight values generally increase under overpressure conditions. Many researchers use normal compaction trend (NCT) by using Bowers (1995)'s and Eaton (1972)'s methods to calibrate the pressure data to well logs, and they use Dix equation or dry bulk moduli and effective stress coefficients, which are

fundamental acoustic behaviors of the rock to calibrate the seismic data to determine overpressure zones. In this work, drilling reports indicate that the predicted overpressure locations have larger mud weights. Identified potential overpressure depths from mud weight changes were correlated and calibrated with well logs. In normal compaction, density and velocity have lower values in an overpressure area with compaction disequilibrium than they should be (Dutta, 2002; Yosandian et al., 2014).

In an overpressured zone, acoustic impedance shows lower values (Badri et al., 2000). To get acoustic impedance as a seismic attribute, we applied model based inversion in this study. Prior to the inversion process, we performed some pre-processes such as wavelet extraction, well correlation (well-tie), horizon determination and picking.

To obtain a pressure map, mud weight changes were calibrated with well log responses. After that, the pressure values that come from mud weight were calibrated with acoustic impedance from logs. Using this calibration, a pore pressure map was obtained by calibrating with acoustic impedance from a model-based inversion.

Seismic approach, well log analysis and 3D pore pressure map were used to identify overpressure zones in Kupe Field, in Taranaki Basin. The pore pressure map was obtained from calibration of pressure and acoustic impedance.

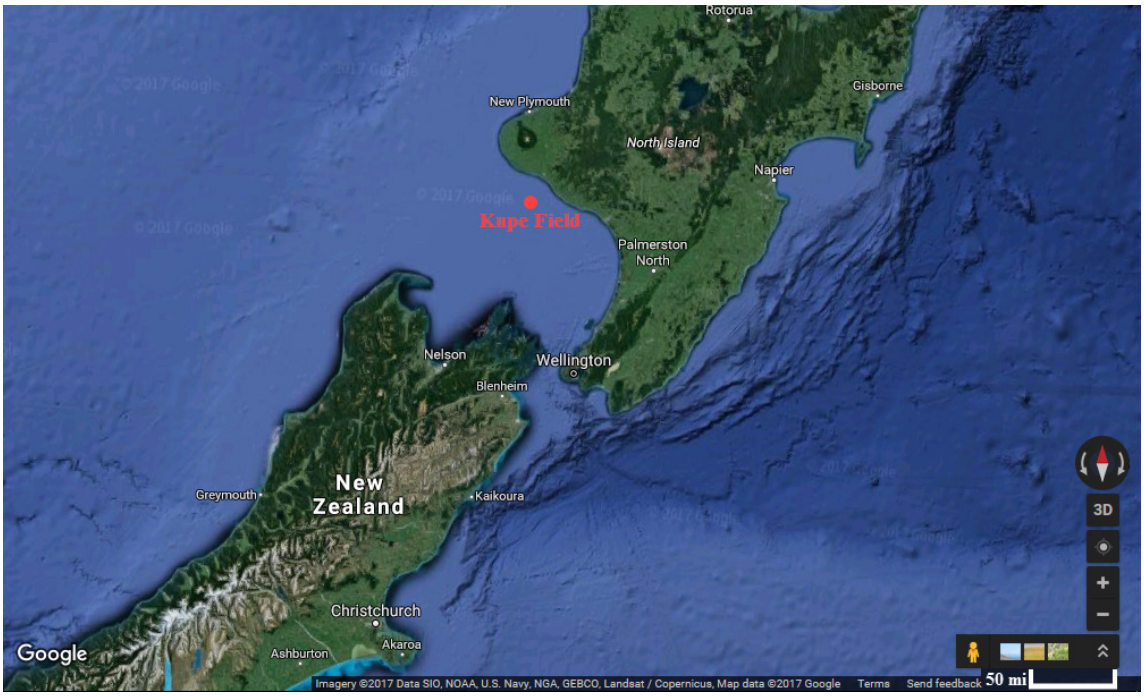

Figure 1.1: Location of Kupe Field (©2017 Google Image Landsat, used with permission, documentation seen on page 47).

2. Geology and Overpressure

Kupe Field is located in the Eastern Mobile Belt of the southern Taranaki basin. The belt has different types of structures such as overthrusts, reverse faults and inversion structures. Taranaki basin is mostly offshore and covers 100,000 km^2. To date, 1.8 billion bbl of oil have been discovered in the basin. Important trap types are inversion anticlines, overthrusts and fault-dependent closures (Webster et al., 2010).

The Kapuni Group that is the main delta system was established in Taranaki basin. A coastal system from northeast-southwest and west-east feeds the group (Matthews and Lewis, 2001). The Mangahewa and Farewell Formations are the fluvial sediments of Kapuni Group are the reservoirs of Kupe gas condensate field (Webster et al., 2010).

Active tectonics, period of high sedimentation rate, horizontal stress and rapid generation of gas in low permeability are the contributors to overpressure in this basin (Webster et al., 2010).

The definition of overpressure is that formation pressure is higher than hydrostatic pressure. Each formation includes the pore spaces which fluids occupy. Formation pressure or pore pressure is the pressure that exists on these fluids. The weight of the fluid column causes another pressure that is described as hydrostatic pressure.

Loading and unloading mechanisms are the main causes of overpressure. The dominant cause of geopressure in sedimentary basins is compaction disequilibrium which is one of a loading mechanism (Hubbert and Rubey, 1959). According to the study by Webster et al. (2010), the pressure data from many sources, including wireline logs, is most consistent for compaction disequilibrium as the reason for overpressure in Taranaki

basin. The author also claims that overpressured shales in the area, overpressures in Manaia Graben and Otaraoa Formation have similarities. This similarity indicates that the dominant cause of overpressure in Taranaki Basin is compaction disequilibrium.

In normal compaction, porosity decreases with expelling pore fluid. During burial, fluid expulsion causes overburden stress. Normal compaction occurs with a slow rate of sedimentation. In this situation, there is balance between increasing overburden stress and expelling fluids (Mouchet and Mitchell, 1989). Hydrostatic pressure is generated by normal compaction in the formation. Under the situation of rapid compaction or low permeability, fluids can be partially discharged. Thus, all or part of the weight of overburden sediments must be supported by the remaining fluids. This situation is the cause of overpressure. Porosity decreases more slowly with the increasing depth in overpressure zone than it otherwise would. This is called “compaction disequilibrium” or “under-compaction” (Zhang, 2013).

The compaction disequilibrium mechanism presents various features in seismic responses, conventional well log analysis and the results of drilling events such as mud weight change and temperature changes when compared with a normally pressured zone. In a normally pressured zone, porosity shows a decreasing trend under sedimentary compaction. Formation resistivity, density and velocity increase with depth. However, porosity acts an increasing behavior while formation resistivity, density and velocity decrease in an overpressure zone caused by compaction disequilibrium (Dutta, 2002; Yosandian et al., 2014) (Figure 2.1).

The aim of this study is to identify overpressure zones in Otaraoa Formation in Kupe field by predominantly examining seismic responses such as acoustic impedance for three wells. Well log responses and the results of drilling events were also taken into account for overpressure zones determination.

In the Otaraoa formation, the lithology of all wells show similarities which means that their overpressure is expected to be similar (Figure 2.2, 2.3 and 2.4).

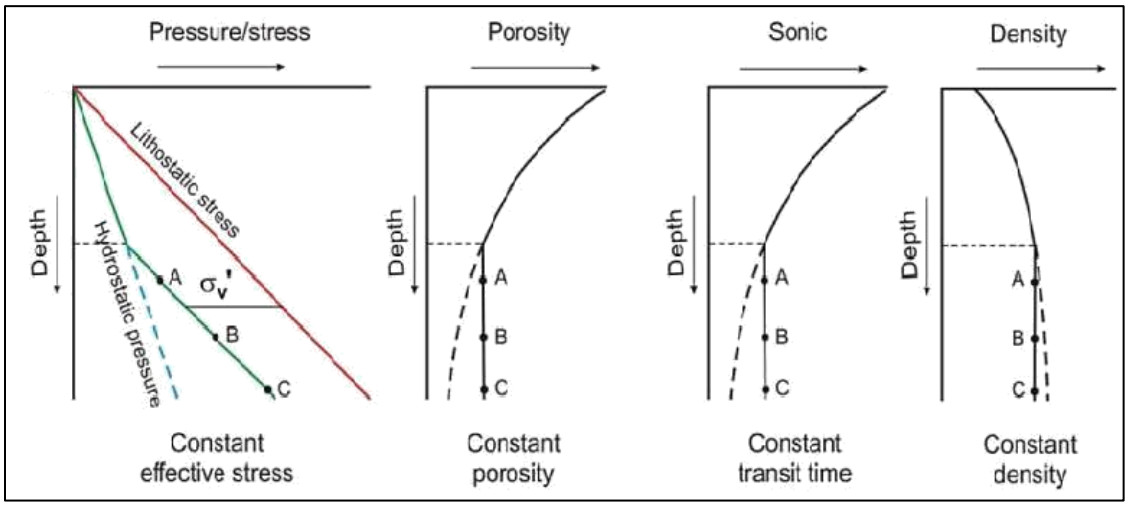

Figure 2.1: The responses of well logs to loading mechanism (Ramdhan et al., 2011) (used with permission, documentation seen on page 48).

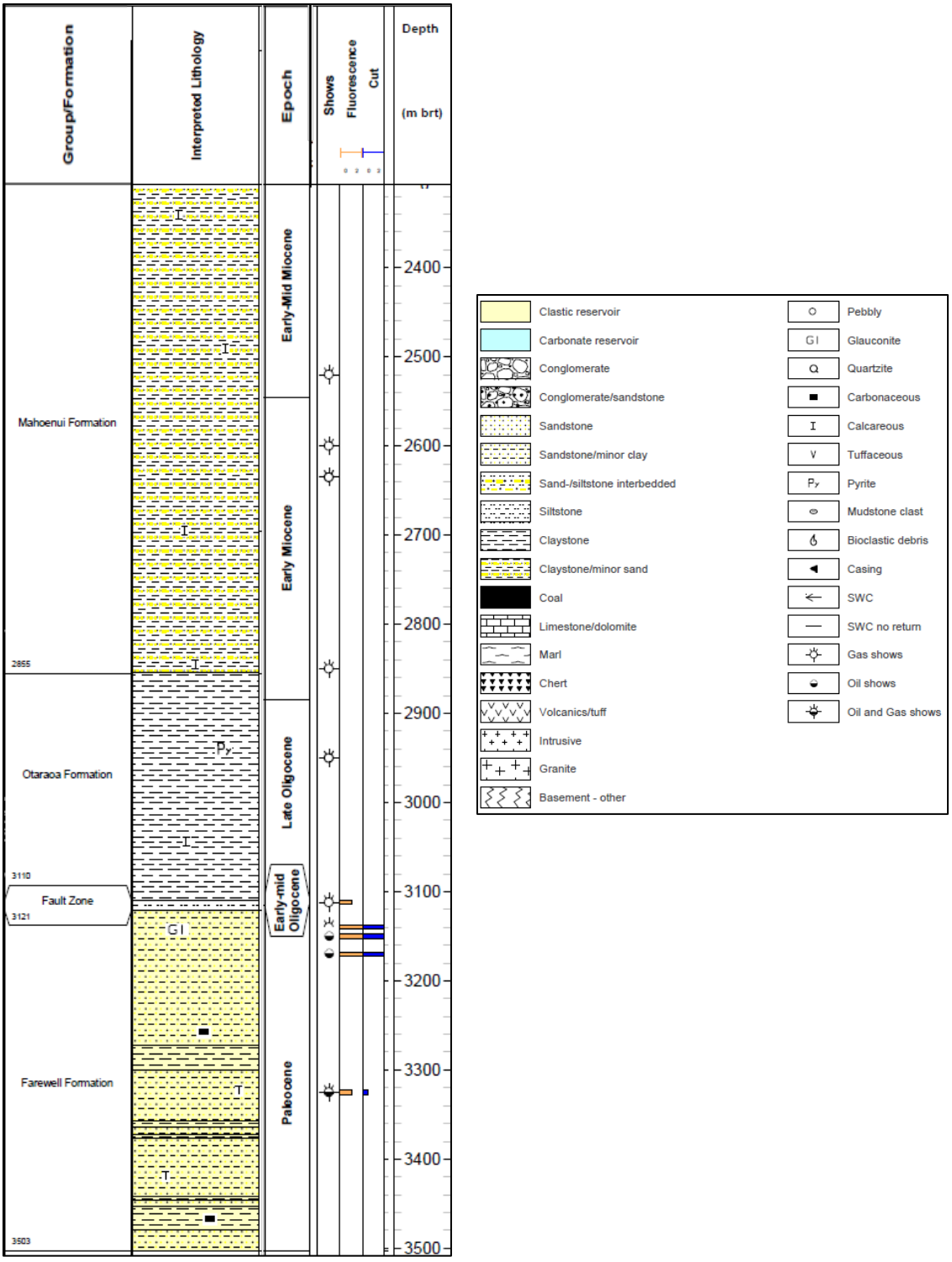

Figure 2.2: Stratigraphy of Otaraoa formation where overpressure occurs, and nearby formations for Kupe South-1 well (Matthews and Bennett, 1987). (GNS Science, used with permission, documentation seen on page 47).

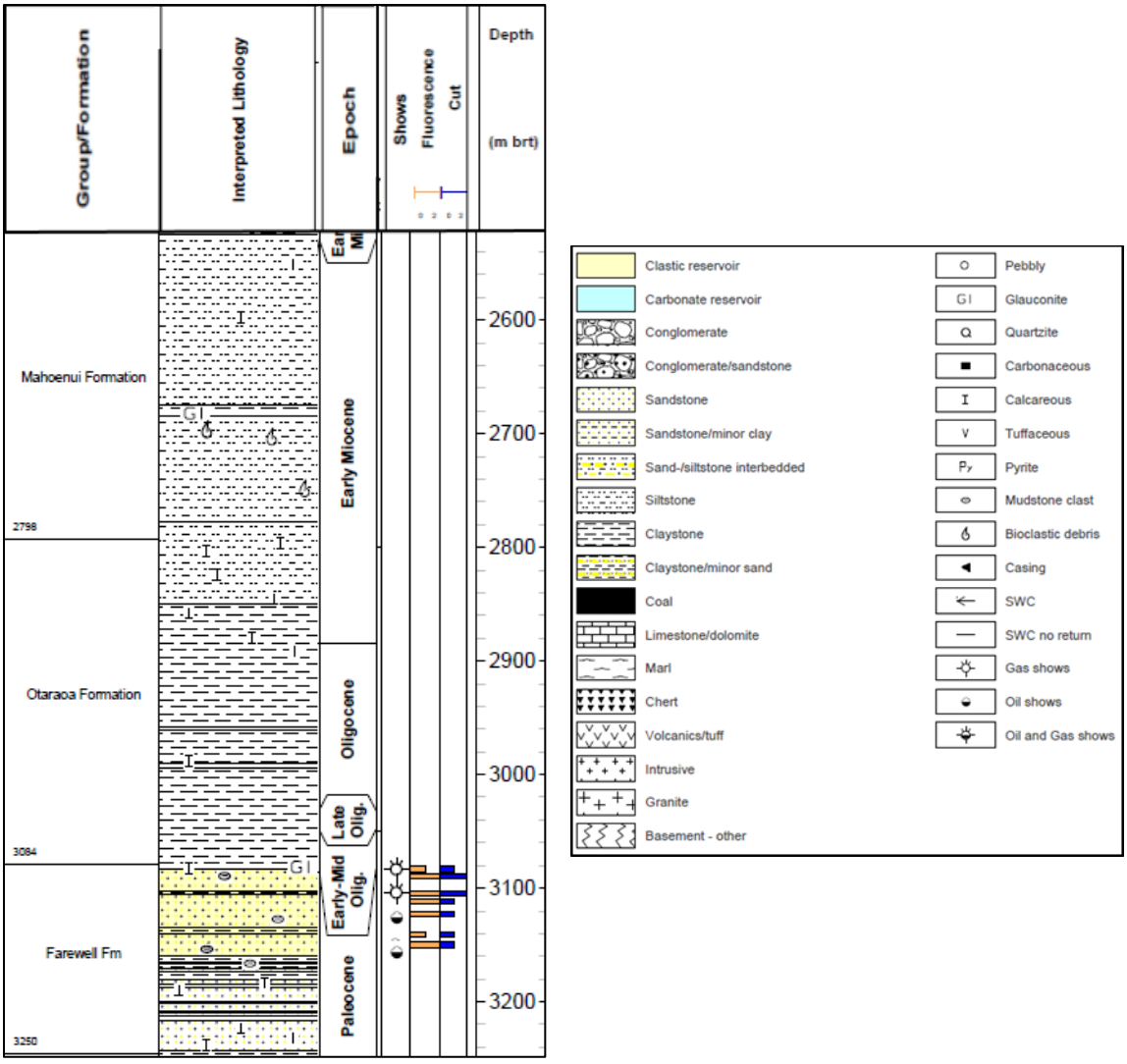

Figure 2.3: Stratigraphy of Otaraoa formation and nearby formations for Kupe South-2 Well (Donaldson et al., 1987). (GNS Science, used with permission, documentation seen on page 47).

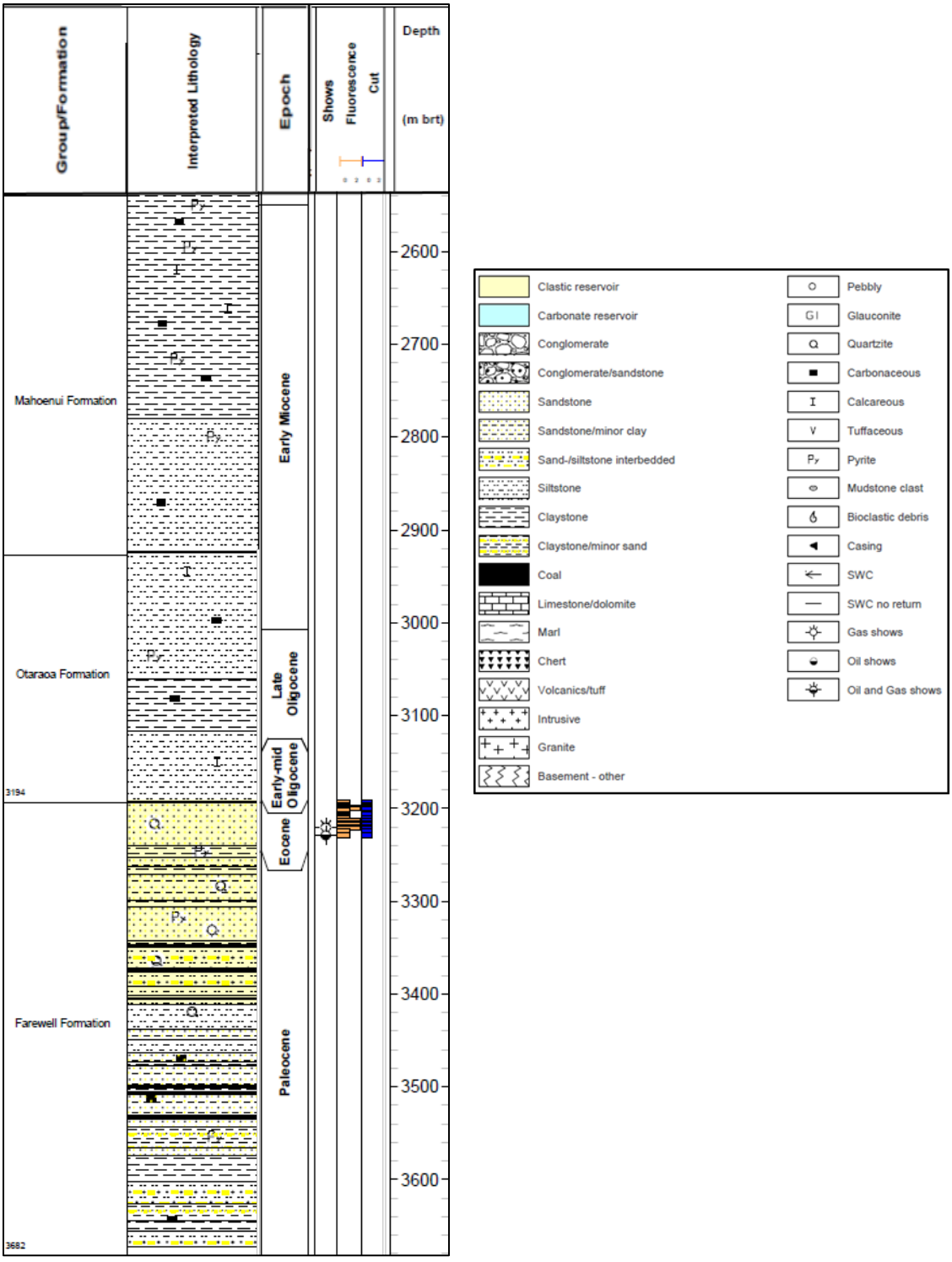

Figure 2.4: Stratigraphy of Otaraoa formation and nearby formations for Kupe-1 well from well completion report (Shell BP Todd Oil Services Limited, 1976). (GNS Science, used with permission, documentation seen on page 47).

3. Methodology

In this section, some information about seismic data before processing will be given. Each step in processing, both seismic and well data to obtain acoustic impedance and overpressure data will be presented.

3.1. Seismic Data

In this study, Kerry 3D marine seismic data, which was acquired in the Taranaki basin in 1996 was used. The survey covers approximately 555 square km. However, some part of the survey was rejected in Hampson Russell Software to focus on the wells that were used in this study. The new seismic data have 81 inlines (620-700) and 101 crosslines (350-450). The record length of the data is 5 ms, and the sample interval is 2 ms. Low cut and high cut frequencies were determined as 3 Hz/18 dB and 180 Hz/70 dB during recording.

The raw data was processed by the marine department of the Perth Processing Center in 2004, and the post-stack data was obtained. Applied processes on raw data were summarized in Figure 3.1. Spectral content of the data between 1600-2600 ms time range was also presented in Figure 3.2 because seismic data quality drastically changes beneath 1600 ms (Figure 3.18). My investigation area is also in this range.

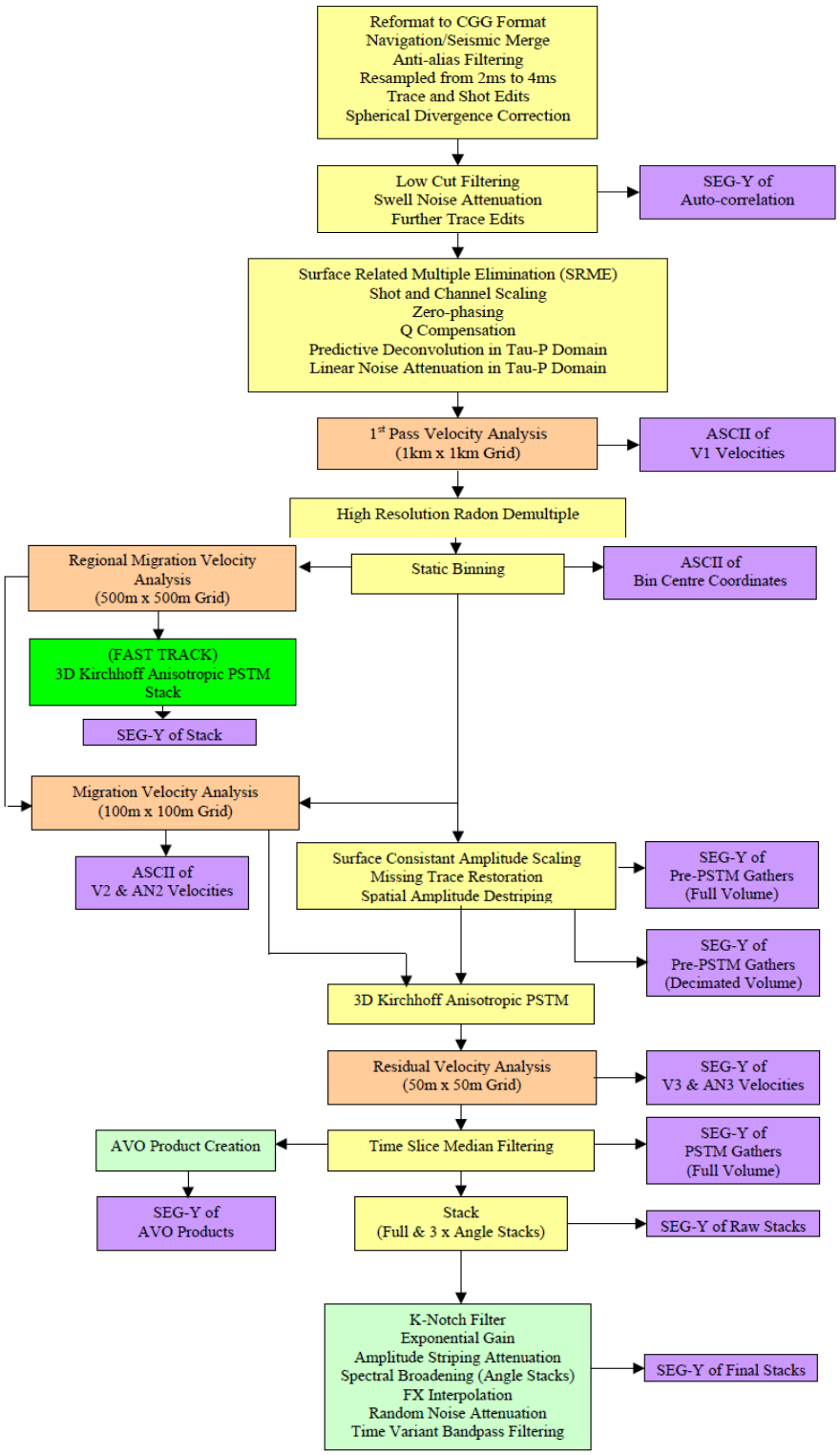

Figure 3.1: Flow Chart of Processing (CGG Australia Services Pty Ltd, 2004) (GNS Science, used with permission, documentation seen on page 47).

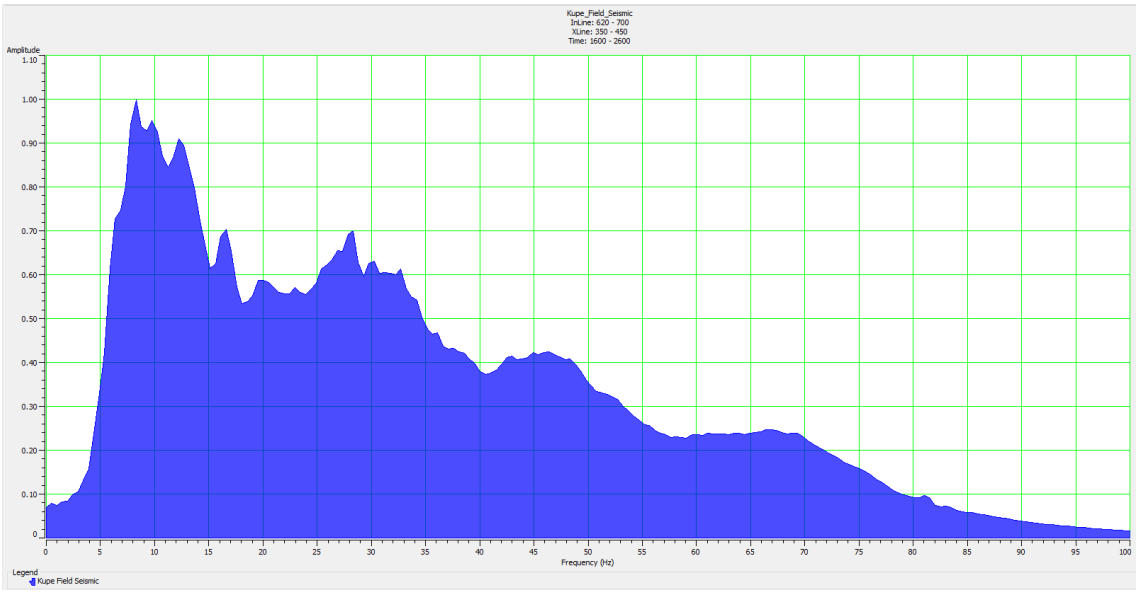

Figure 3.2: Spectral content of final stacked seismic data between 1600-2600 ms time range. 4-8 Hz cutoff frequency was chosen for modeling process.

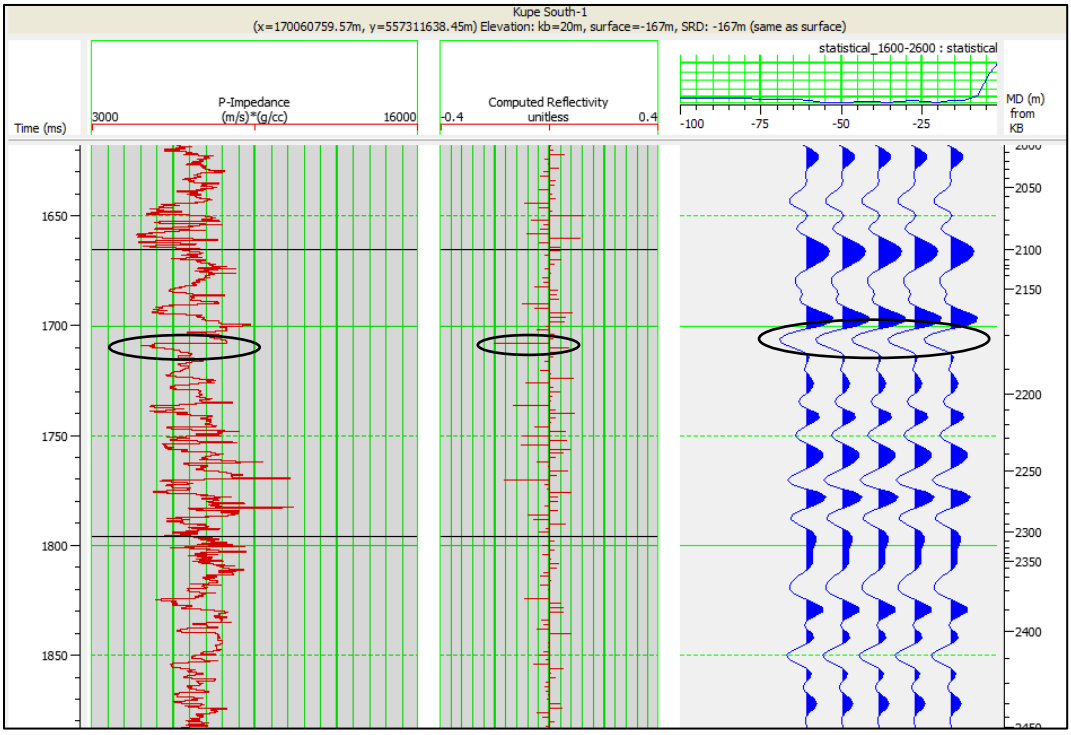

Figure 3.3: When the acoustic impedance decreases, reflectivity becomes negative, and seismic data shows trough. This means that the seismic data has American polarity.

3.2. Well Log Data

In this study, three wells named Kupe South-1, Kupe South-2 and Kupe-1 were used for inversion processing, overpressure determination and pressure calibration. Seven-sample median filter was applied to density and sonic logs to get rid of spikes (Sample interval = 0.15 m). As mentioned in the previous chapter, density and velocity increase with depth. In an overpressured zone, they become constant, or start decreasing (Sonic and velocity are inversely proportional).

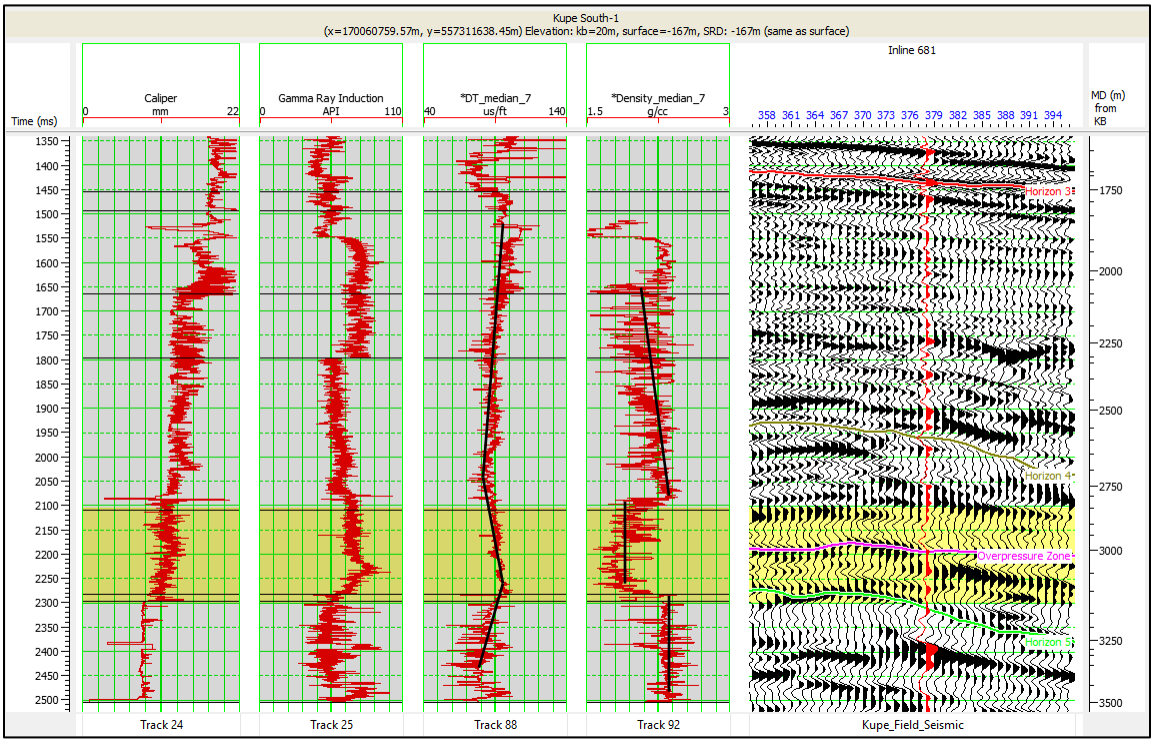

Figure 3.4: Caliper in mm, gamma ray that was accompanying the induction log in API, sonic in µs/ft, density in g/cc, and seismic log is shown in sequence. Red curve on the seismic data shows the nearest curve to the Kupe South-1 well. Yellow highlighted area is Otaraoa Formation which is overpressured zone. Sonic increases, and density decreases in this zone.

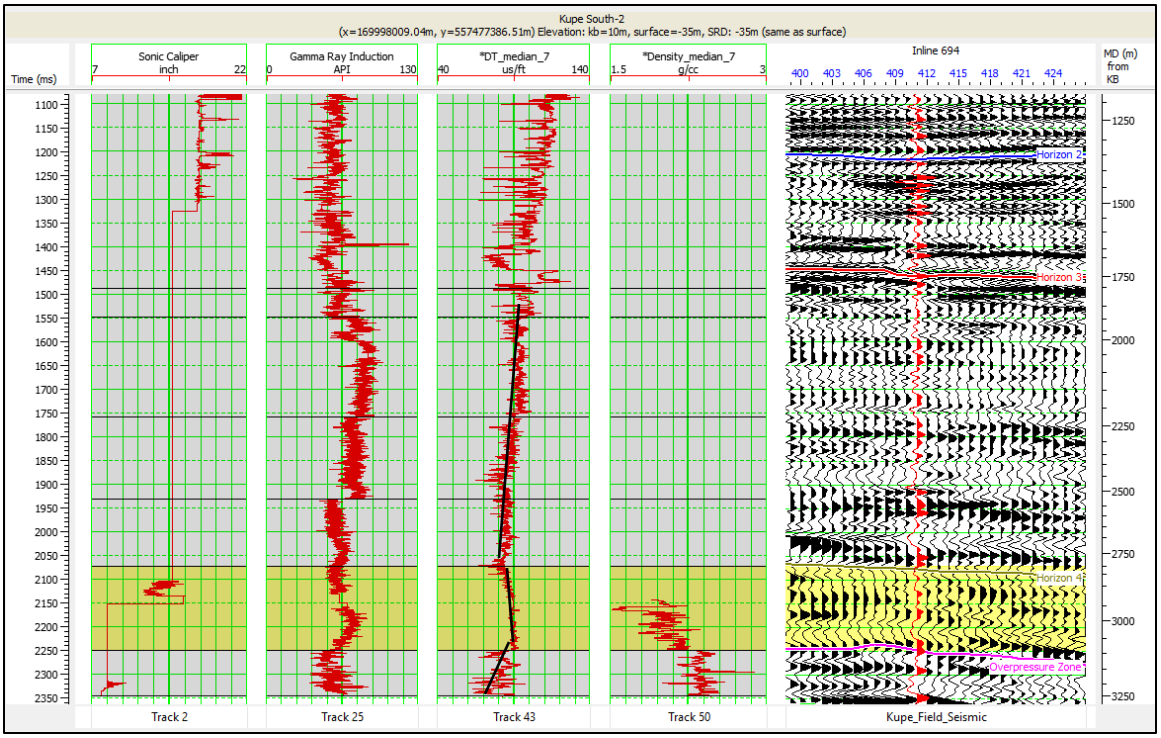

Figure 3.5: Sonic caliper in mm, gamma ray that was accompanying the induction log in API, sonic in µs/ft, density in g/cc, and seismic log is shown in sequence. Red curve on the seismic data shows the nearest curve to the Kupe South-2 well. Yellow highlighted area is Otaraoa Formation which is overpressured zone. Sonic log increases in this zone but we cannot make comment about density data because it is insufficient. We can only say that average density in this formation is low, and close to Kupe South-1 well.

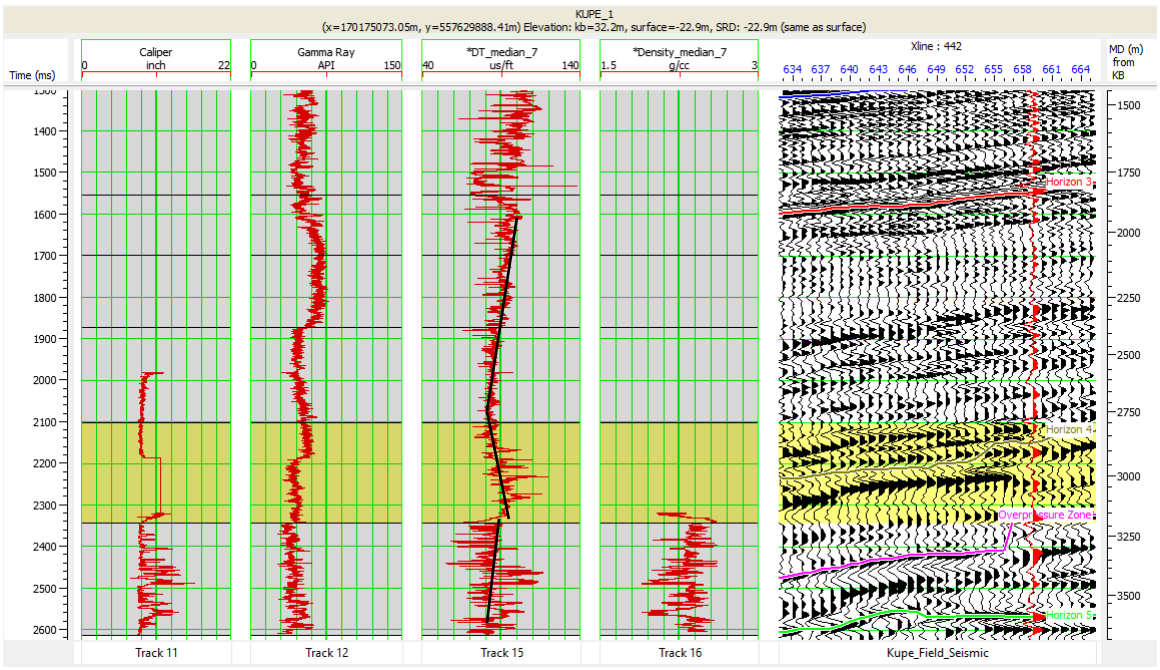

Figure 3.6: Sonic caliper in mm, gamma ray in API, sonic in µs/ft, density in g/cc, and seismic log is shown in sequence. Red curve on the seismic data shows the nearest curve to the Kupe-1 well. Yellow highlighted area is Otaraoa Formation which is overpressured zone. Sonic log increases in this zone but we cannot make comment about density data because it is insufficient.

3.3. Methods

Seismic inversion has a significant role for determining overpressure by using seismic and well log data. The original 3D seismic survey covers the large area (214 sq mi). That's why, it was cropped, and Kupe Field which is close to overpressure well was put in rectangle.

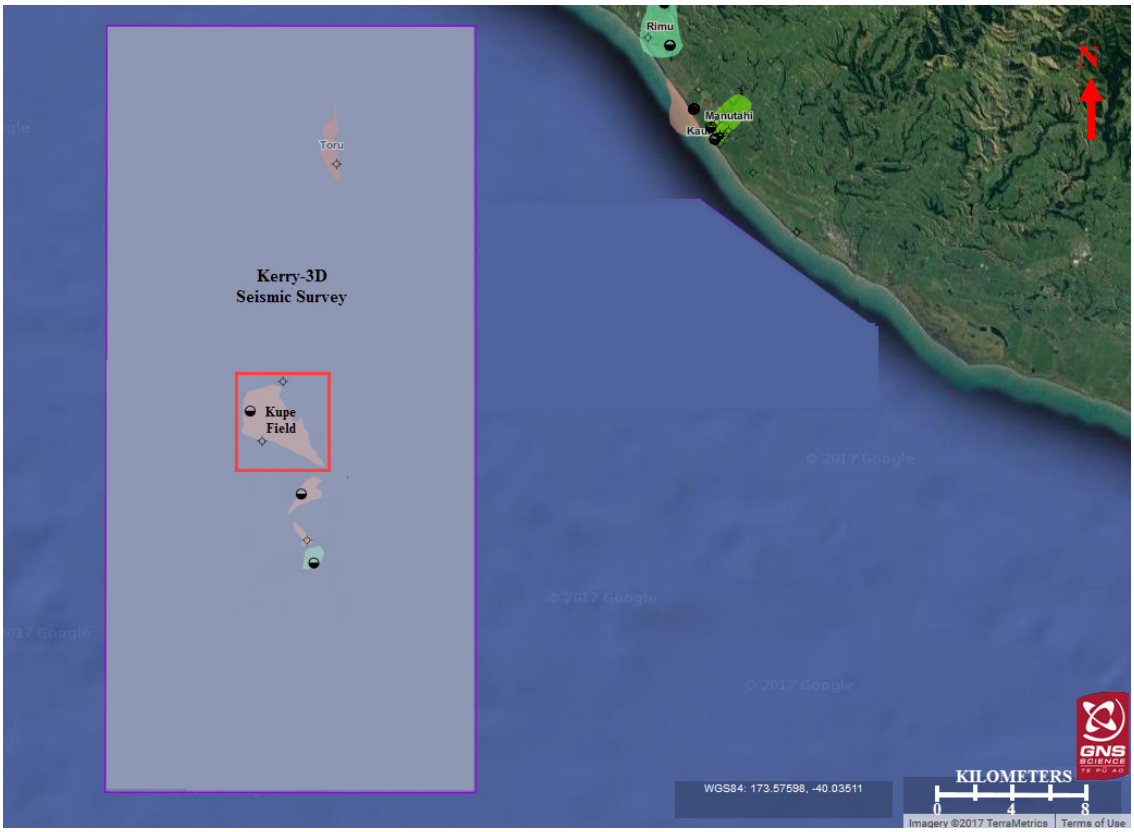

Figure 3.7: Purple rectangled area is Kerry-3D seismic survey which cover 37 x 15 km^2 (214 sq mi) that consists of 736 crossline and 288 inline seismic section. Red rectangled area is Kupe Field. Pink color shows gas and condensate which is explored in this field. (modified from Google Maps and GNS Science and Petroleum Basin Explorer (PBE) Map, ©2017 Google Image Landsat) (used with permission, documentation seen on page 47).

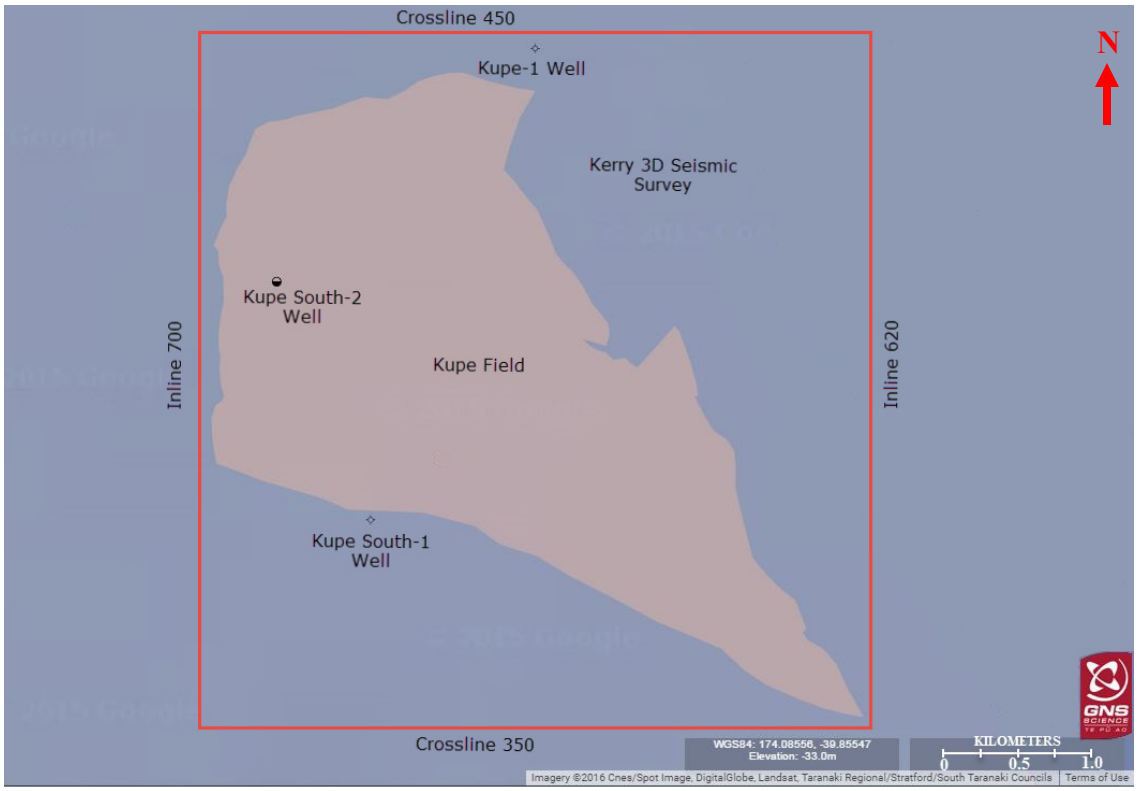

Figure 3.8: Rectangle that covers Kupe Field was used. Pink color shows gas and condensate which is explored in this field. The area in rectangle has 81 inlines and 101 crosslines which cover 6.5 x 5 km^2 (12.5 sq mi). (modified from Google Maps and GNS Science and Petroleum Basin Explorer (PBE) Map, ©2016 Google Image Landsat) (used with permission, documentation seen on page 47).

The 3D Seismic data and well log data (Kupe South-1, Kupe South-2 and Kupe-1) was loaded into the Hampson Russell Software to do seismic processing. These processes are wavelet extraction, well correlation (well-tie), horizon determination and picking, model based seismic inversion, and the calibrating mud weight to well logs and inversion data.

A checkshot file for each well loaded to provide correlation between seismic and well data. A median filter was applied to sonic and density logs for all wells to get rid of spikes. Ricker and statistical wavelets were created to correlate the wells, and determined

which wavelet is the best fit for the correlation. Getting the best correlation coefficients, we utilized well tie process after extracting the wavelets. A horizon picking process was then applied according to appropriate seismic traces and possible overpressure zone boundaries. After these preprocess steps, a model based inversion that is one of the deterministic inversion methods was applied to the data to get acoustic impedance values. The best match model with the synthetic data and the real data is acquired by the iteration model based inversion (Barclay, 2008). A primary model is created for all wells and horizons, and inversion was performed for all volume of seismic data.

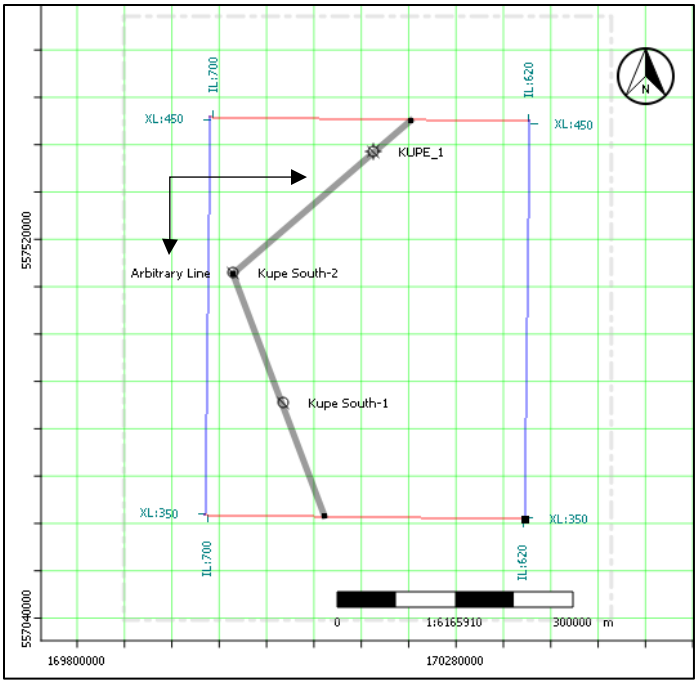

Figure 3.9: Geometry of the seismic data, location of the wells on the survey and arbitrary line which passes on all three wells.

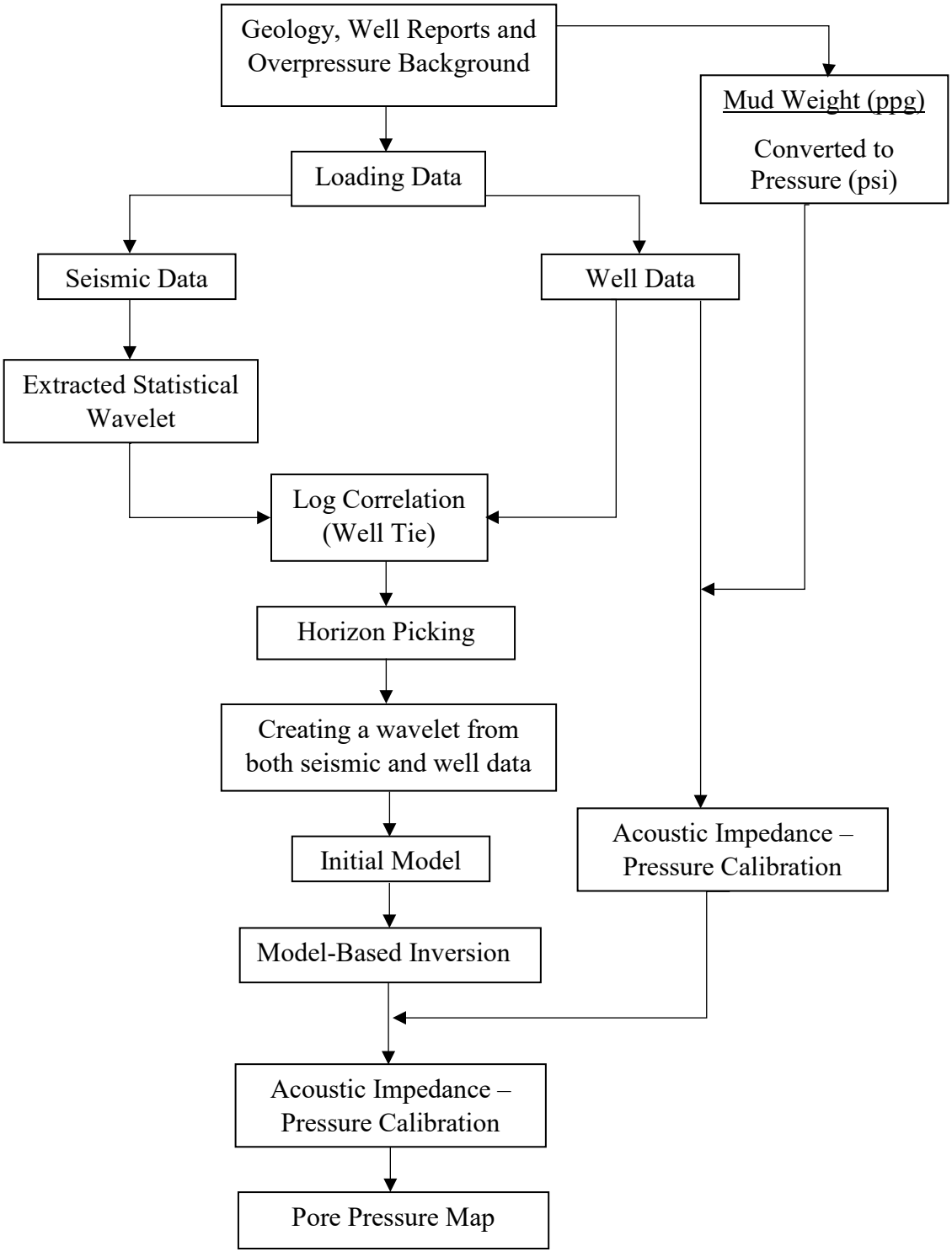

Figure 3.10: Workflow of this study.

3.3.1. Creating Wavelets

Extracting wavelet is useful for correlating the wells and inversion processes. For this study, statistical wavelet was extracted within the range of 1600-2600 ms because seismic data, and Ricker wavelets whose dominant frequencies are 15 Hz, 20 Hz, 25 Hz and 30 Hz were created. In the log correlation process, all of these wavelets were compared to each other, and statistical wavelet had a higher correlation coefficient which shows the matching rate between synthetic data and seismic data than the others. That's why, a statistical wavelet was used for the log correlation. After the log correlation, a new wavelet was created by using both seismic and well data within the range of 1600-2600 ms to use in each step of the inversion processes.

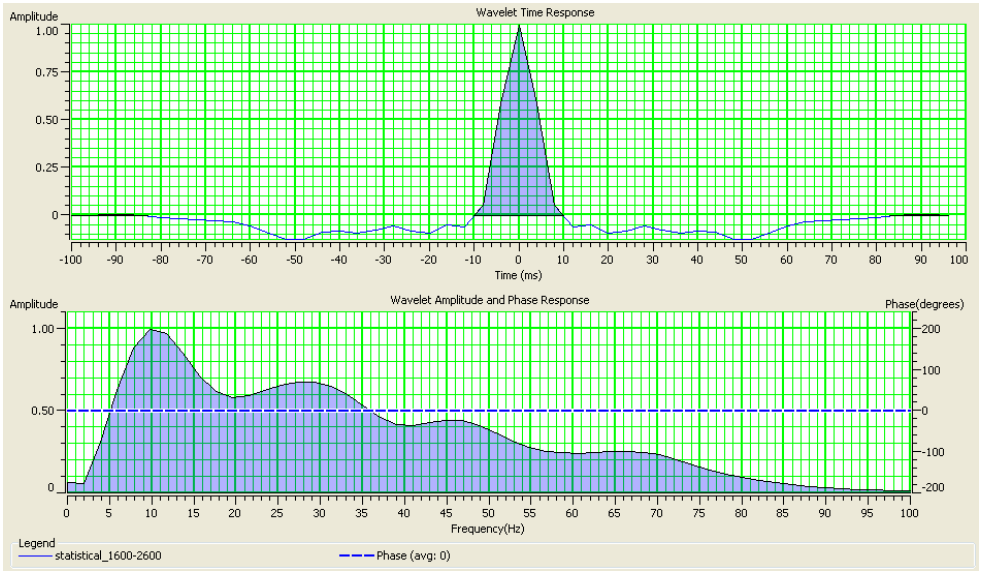

Figure 3.11: Extracted statistical wavelet between 1600-2600 ms time range.

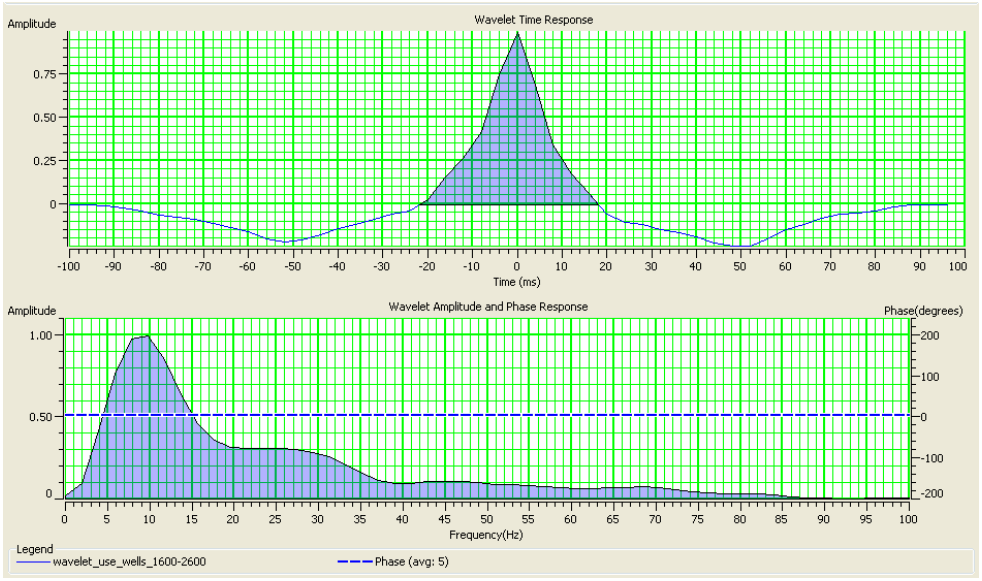

Figure 3.12: Extracted wavelet by using seismic and well logs between 1600-2600 ms time range after well-tie process.

3.3.2. Log Correlation (Well Tie)

Before starting the correlation, check-shot corrections were made for each well. The synthetic trace also needed shifting based on the seismic trace. After shifting process for each well, correlation coefficient values were lower than 0.25. Extracted wavelets were tried one by one, and determined that the statistical wavelet gave higher coefficient values than the Ricker wavelets. By using the statistical wavelet for all wells, squeezing and stretching processes was applied until obtaining good correlation coefficient results. During this process, we tried to keep depth intervals equal. As a result, correlation coefficient values of 0.49 from Kupe South-1 well, 0.57 from Kupe South-2 well, and 0.62 from Kupe-1 well were obtained.

Sonic and density logs, and a seismic wavelet are used to generate synthetic seismograms. The density log covers between 1865 and 3500 m for Kupe South-1 well,

2935 and 3250 m for Kupe South-2 well, and 3145 and 3665 m for Kupe-1 well. Insufficient density data has a negative impact on getting higher correlation results. Gardner's equation was used to obtain density for the missing density logs of Kupe South-2 and Kupe-1 well by using the sonic log. However, it is not capable of producing the results in the overpressured zone for the well where we have such information. Therefore, we cannot use it away from the well either.

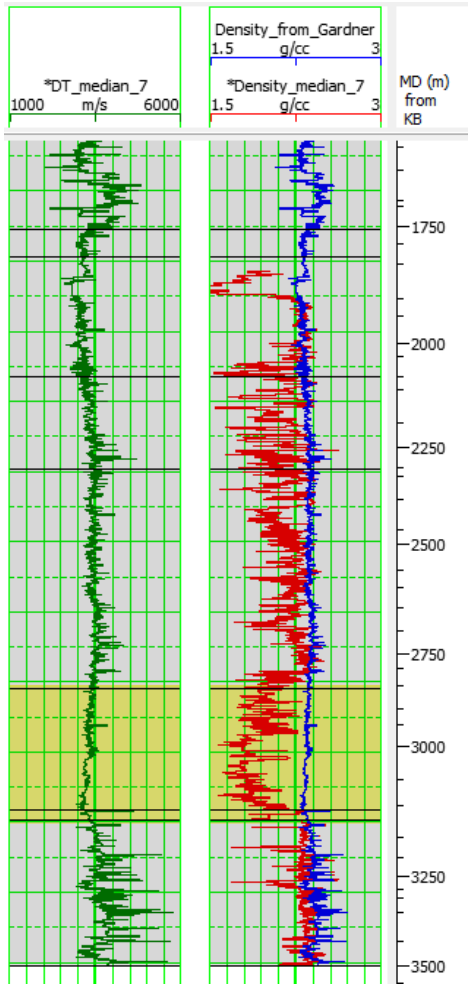

Figure 3.13: Sonic and density logs of Kupe South-1 well. Green curve on the left is sonic log. Red curve is original density, and the blue curve is the density that was obtained from Gardner's Equation by using sonic log. It is easily seen that, density log from Gardner's equation is not reliable in overpressure zone which is yellow highlighted area.

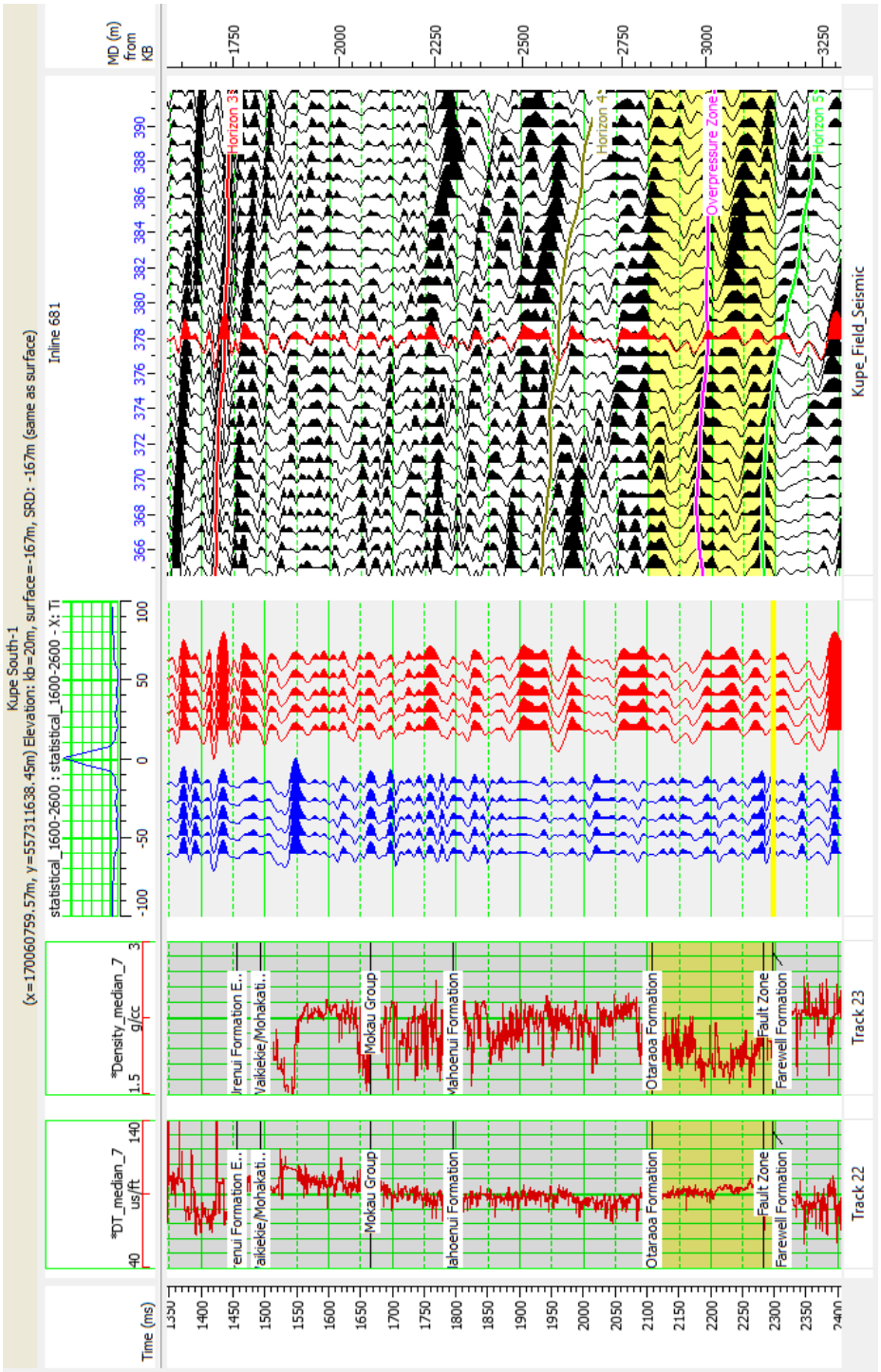

Figure 3.14: Log correlation of Kupe South-1 well. In the middle of the graphic, blue traces are synthetic data, red traces are from the original seismic data which is average of inline and crossline. Sonic and density wells are on the left, and original seismic data is on the right. Red trace on the original seismic data is the closest trace to Kupe South-1 well.

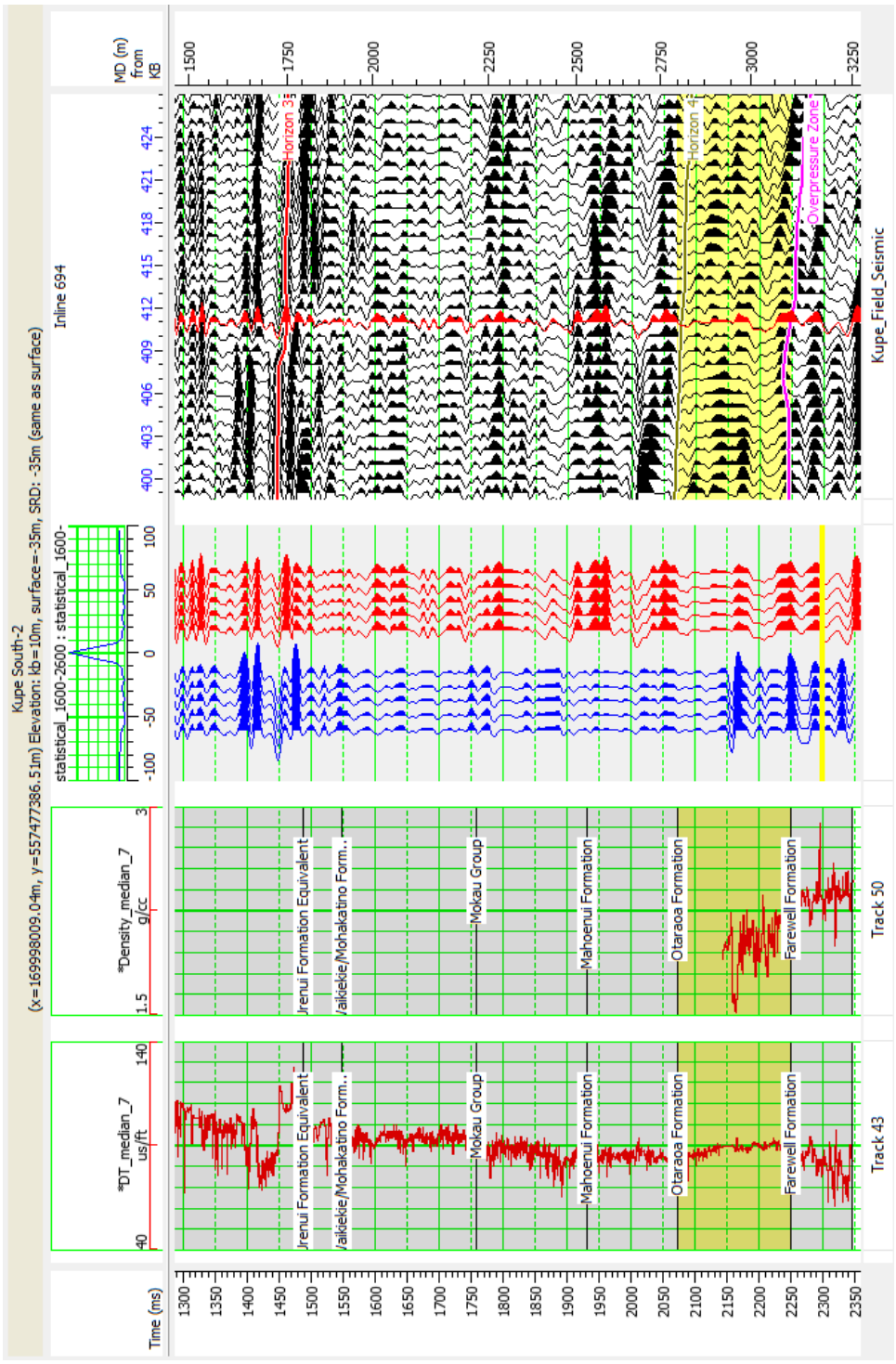

Figure 3.15: Log correlation of Kupe South-2 well. In the middle of the graphic, blue traces are synthetic data, red traces are from the original seismic data which is average of inline and crossline. Sonic and density wells are on the left, and original seismic data is on the right. Red trace on the original seismic data is the closest trace to Kupe South-2 well.

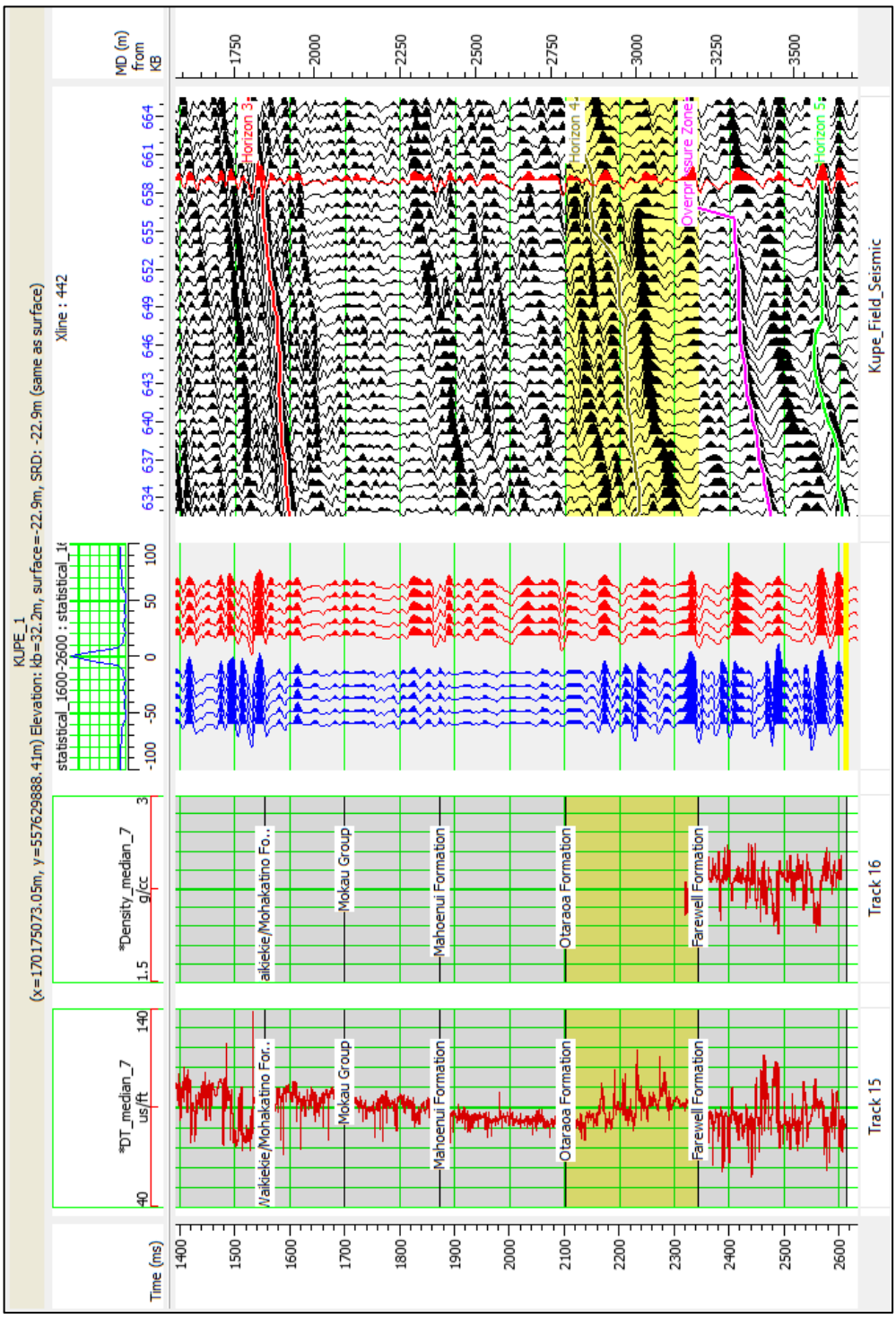

Figure 3.16: Log correlation of Kupe-1 well. In the middle of the graphic, blue traces are synthetic data, red traces are from the original seismic data which is average of inline and crossline. Sonic and density wells are on the left, and original seismic data is on the right. Red trace on the original seismic data is the closest trace to Kupe-1 well.

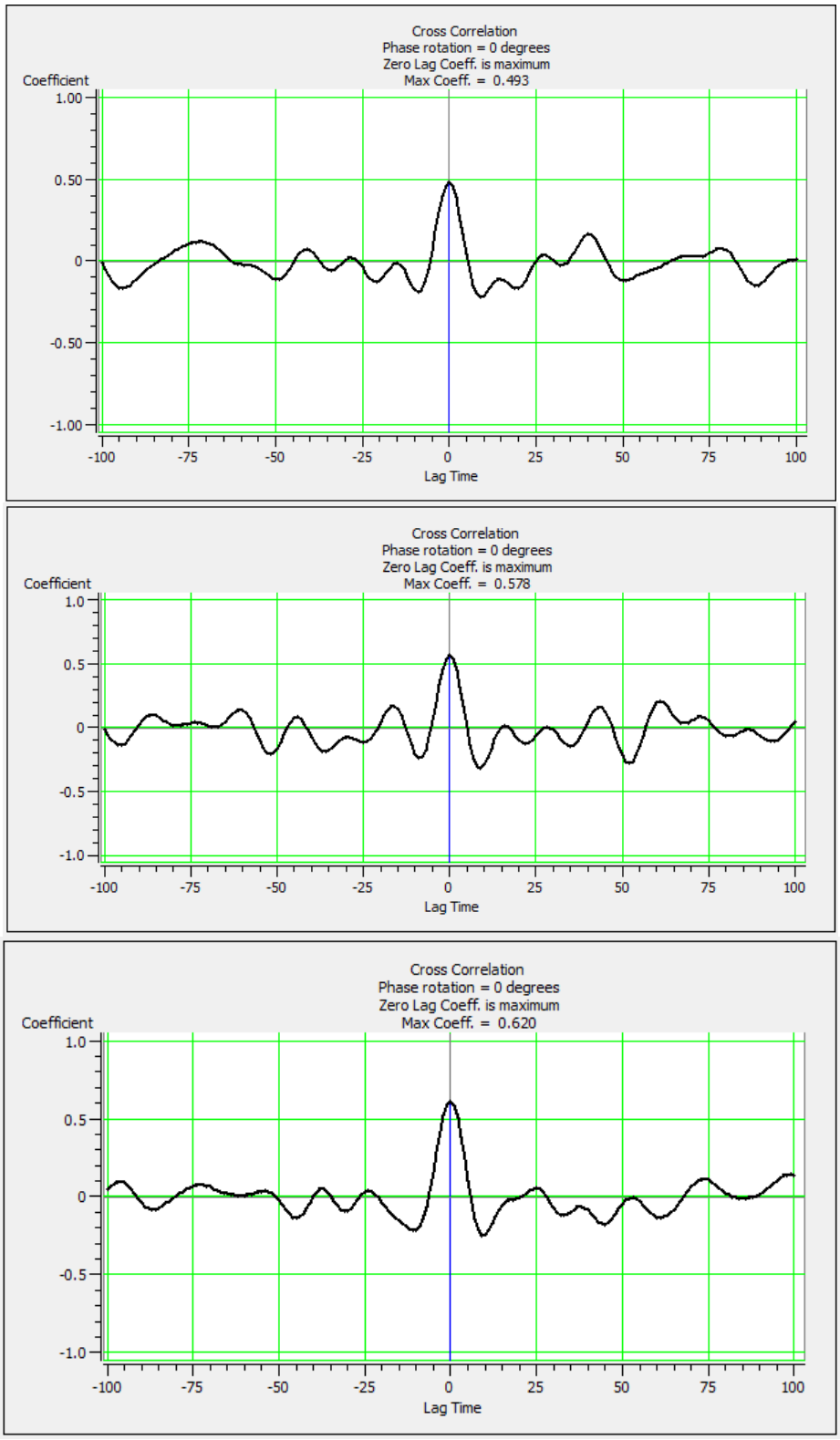

Figure 3.17: Cross correlation of all three wells after doing well tie. Kupe South-1 has 0.49, Kupe South-2 has 0.57, and Kupe-1 has 0.62 correlation coefficients.

3.3.3. Horizon Determination and Picking

Horizon picking is one of the processes used before seismic inversion. To determine the place of horizons, this information was considered:

1) Good continuous seismic traces
2) Overpressure zone
3) One above overpressure zone, the other one below overpressure zone

Even though good continuous seismic traces are far from the overpressure zone, three horizons (horizon-1, horizon-2 and horizon-3) were determined and picked.

In chapter 2, it is mentioned that Otaraoa formation is an overpressure zone. Mud weight reports in Table 3.1 and well log behaviors in Figure 3.4, 3.5 and 3.6 also support this claim. Near these overpressure zones, seismic data quality is not good but three horizons (horizon-4, horizon 5 and overpressure zone) were chosen and picked.

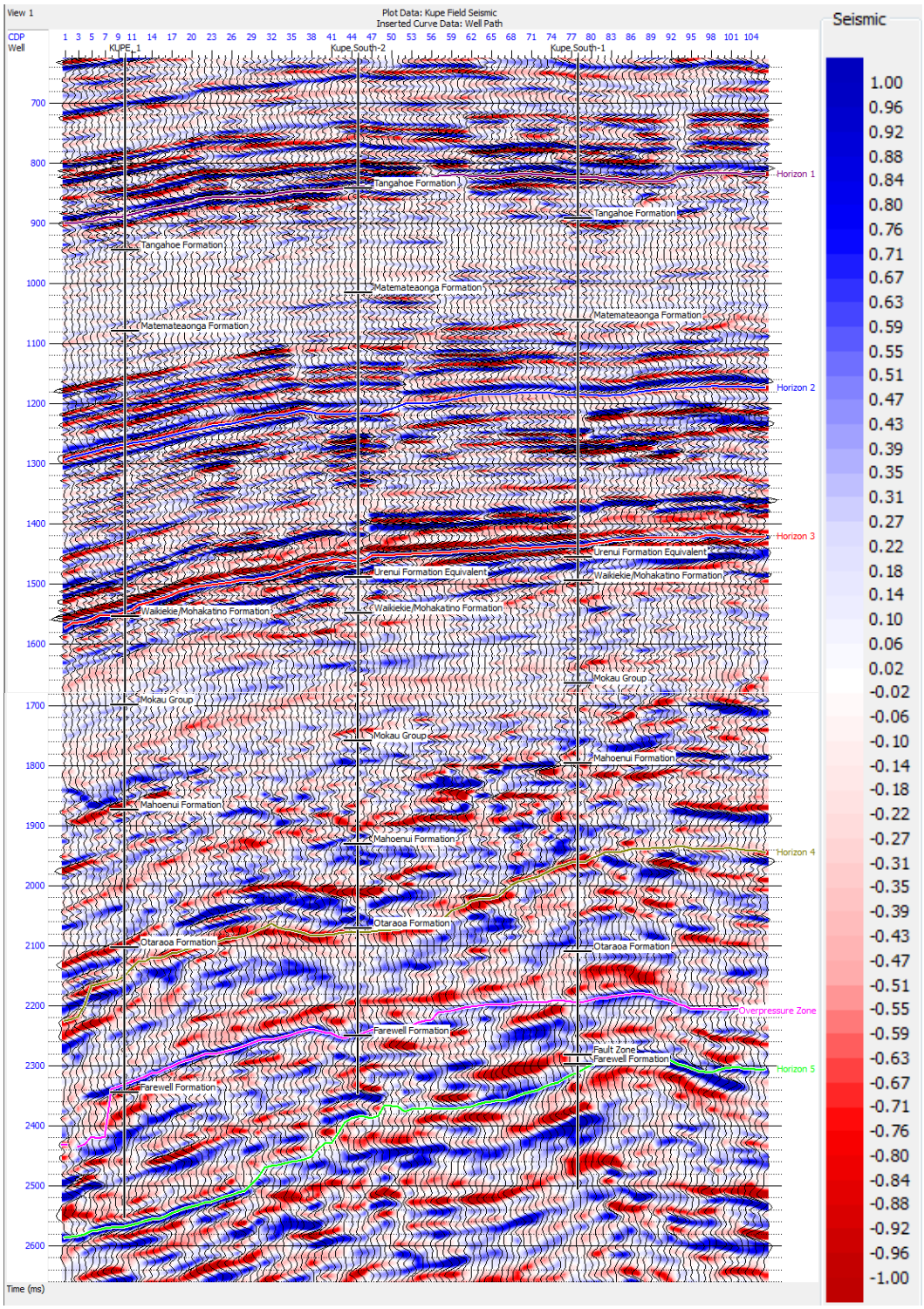

Figure 3.18: Original seismic data from the arbitrary line which includes all three wells with six horizons. Blue color on the seismic data represents peak, red color represents trough. Positive amplitudes which are blue show increase in acoustic impedance that is called American Polarity.

3.3.4. Model Based Post-Stack Inversion

Model based inversion is a type of amplitude inversion, and one of the deterministic inversion methods. A model of layers with densities, thicknesses, estimated formation depths and velocities which are obtained from well logs are used to forward modeling at the beginning of model based inversion. Basically, an acoustic impedance or inverted P wave which is obtained in this study is derived from compressional P wave velocity and density. A modeled synthetic trace is created by a seismic pulse combined with this model. Inversion uses this seismic trace by deleting the seismic pulse to create an earth model for the location of this trace. Most inversion routines repeat modeling to get the best fit model, and to minimize the difference between the synthetic trace and the data (Barclay, 2008).

The inversion processes that were applied in this study are:

- Statistical and Ricker wavelets were created before the log correlation.
- Statistical wavelet was chosen based on coefficient results in the log correlation.
- Log correlations were made for all wells.
- A new wavelet was created by using both seismic and well data.
- 6 horizons were picked.
- An initial model was built by using only Kupe South-1 well due to missing density logs of other wells. 4-8 Hz frequency range was set to obtain initial model (Figure 3.19).
- Inversion was analyzed and applied to all volume of seismic data to obtain acoustic impedance (Figure 3.20 and 3.21).

- Created new wavelet and all horizons were used during initial model and inversion process.

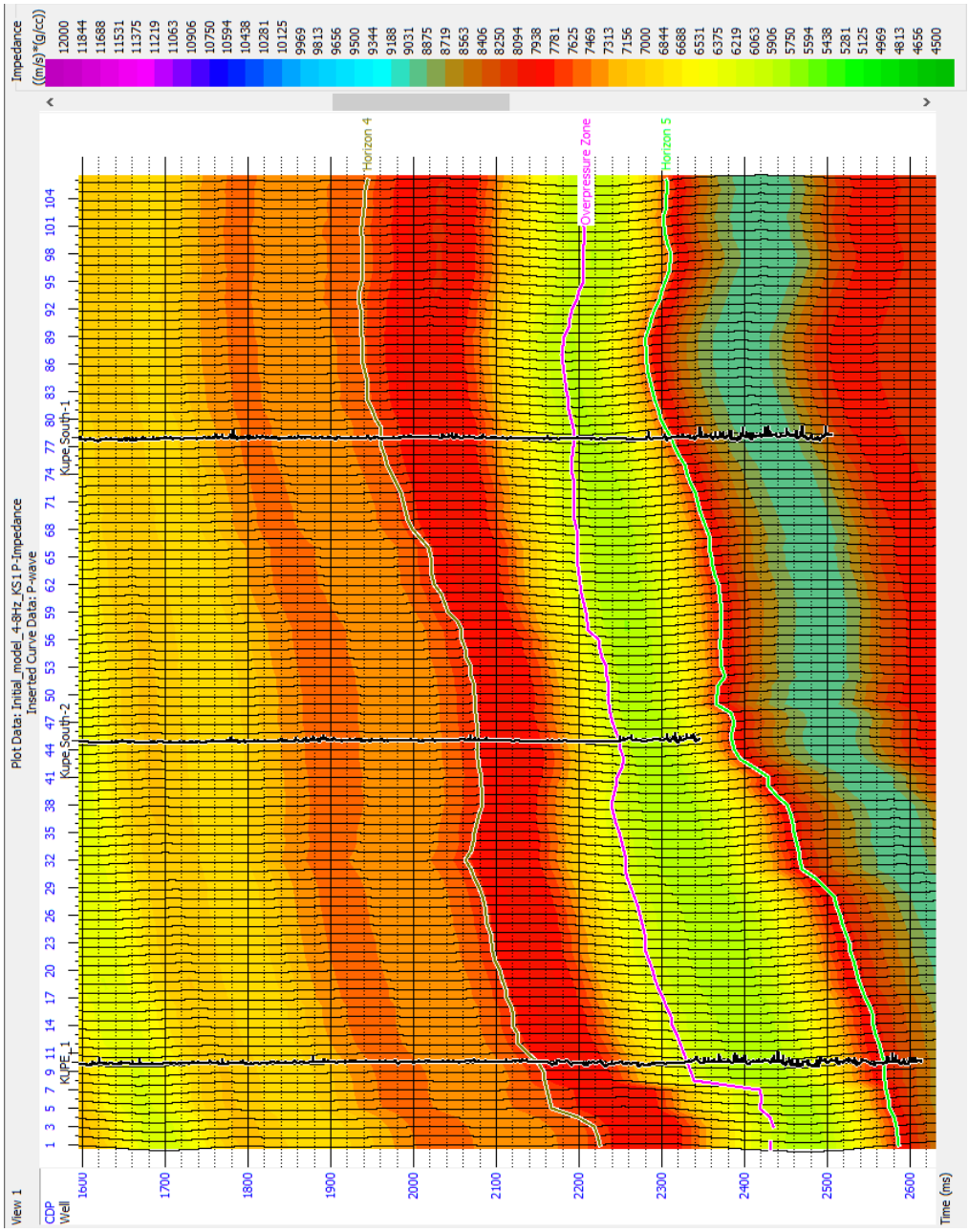

Figure 3.19: Built initial model whose cut off frequency is between 4 and 8 Hz. Kupe South-1 well and the wavelet that was created by using well logs and seismic data was used to build the model.

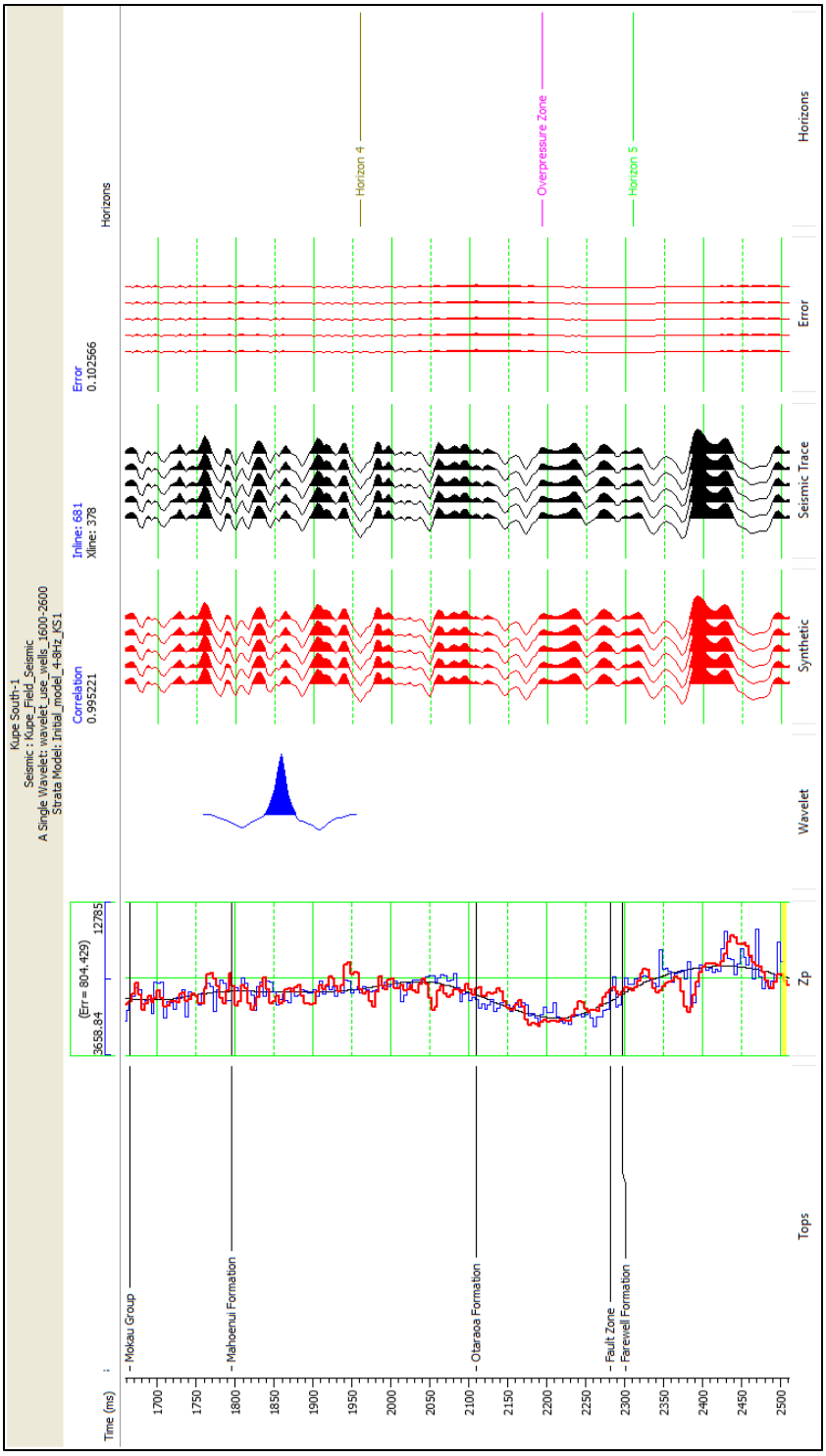

Figure 3.20: Inversion analysis for Kupe South-1 well. 99.5% match on synthetic data after inversion. There is also good match between original log and inverted log in Otaraoa Formation.

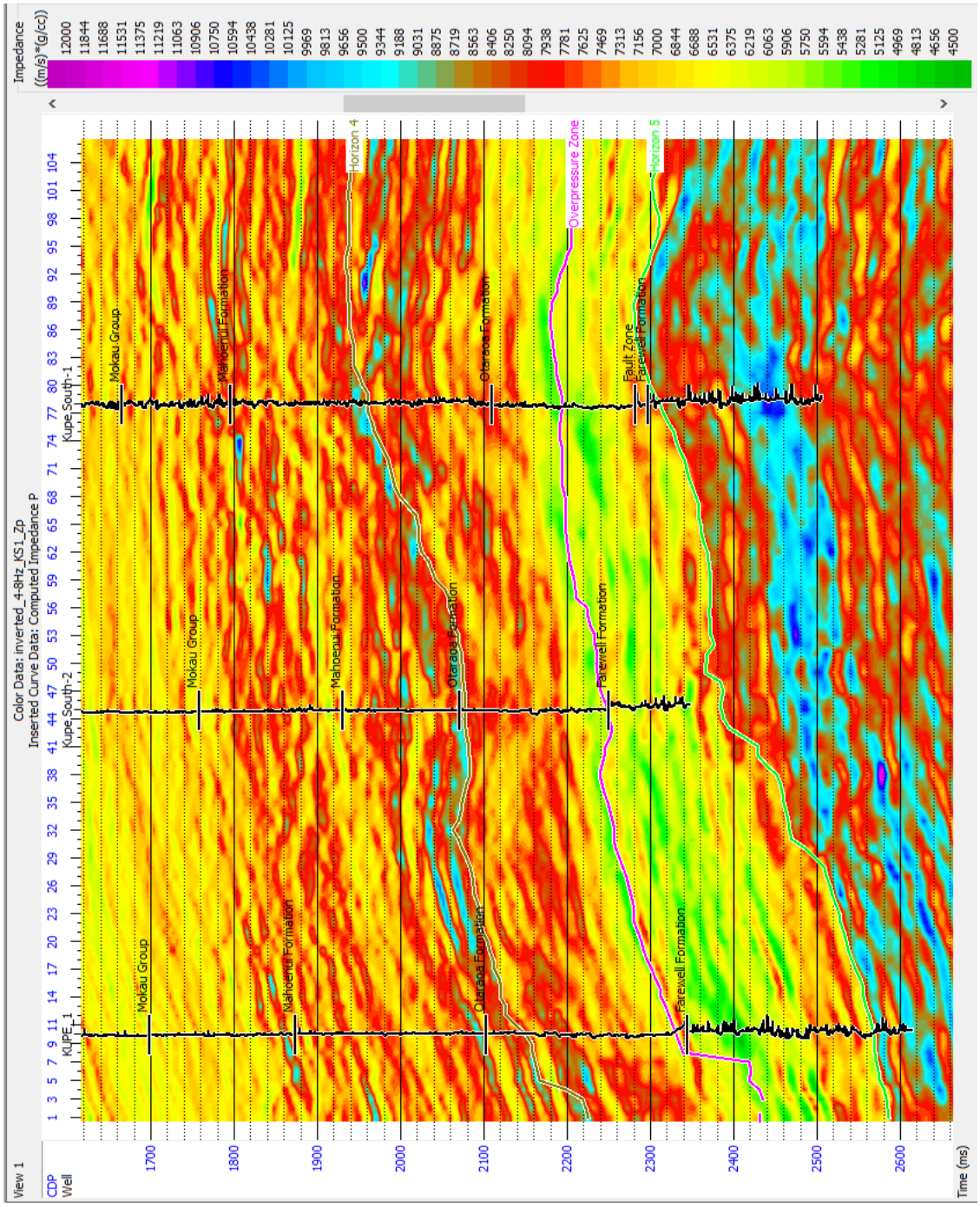

Figure 3.21: Model based inversion result by using only Kupe South-1 well. Green areas below and above of overpressure zone horizon show lowest acoustic impedance.

3.3.5. Pressure Calibration

To obtain a pore pressure map, pressure from mud weights was calibrated with acoustic impedance log of Kupe South-1 well, then the obtained result was calibrated with acoustic impedance from the inversion result. Due to an insufficient density log of Kupe South-2 and Kupe-1 wells, they weren't taken into account for the calibration process.

Table 3.1: Mud weights for Kupe South-1 well (left) and Kupe South-2 well (right) (Matthews and Bennett, 1987; Donaldson et al, 1987). 2803 m from Kupe South-1 well and 2607 m from Kupe South-2 well are tops of overpressure because they suddenly increase at these depths. Kupe-1 well doesn't have mud weight report. Pressure values converted from mud weight by using "Pressure (psi) = Mud weight (ppg) * 0.052 * Depth (m) * 3.281" equation.

Kupe South-1

Depth (m)	Pressure (psi)	Mud Weight (ppg)
168	246.5	8.6
496	727.8	8.6
653	958.1	8.6
810	1243.8	9.0
1350	2165.1	9.4
1619	2624.1	9.5
1690	2739.2	9.5
1820	2980.9	9.6
1892	3066.6	9.5
2086	3381.0	9.5
2166	3510.7	9.5
2298	3842.3	9.8
2435	4112.9	9.9
2564	4549.5	10.4
2701	4884.7	10.6
2813	5111.3	10.65
2888	5420.0	11.0
3008	5645.2	11.0
3072	5765.3	11.0
3118	5851.7	11.0
3142	5896.7	11.0
3153	5917.3	11.0
3184	5975.5	11.0
3271	6138.8	11.0

Kupe South-2

Depth (m)	Pressure (psi)	Mud Weight (ppg)
171	250.9	8.6
650	1020.3	9.2
1284	2015.4	9.2
1519	2410.2	9.3
1737	2756.1	9.3
2607	4136.5	9.3
2955	5444.9	10.8
3037	5596.0	10.8
3083.2	5681.1	10.8
3111.5	5733.3	10.8
3123.2	5754.8	10.8
3151.1	5806.2	10.8
3178.1	5856.0	10.8
3197.8	5892.3	10.8

3273	6142.5	11.0
3325	6126.7	10.8
3428	6199.5	10.6
3503	6335.1	10.6

Kupe South-1 well was chosen to calibrate the mud weight pressure to acoustic impedance of this well because Kupe South-2 well doesn't have an acoustic impedance log in the overpressure zone and above it. An acoustic impedance log was obtained by multiplying density in g/cc and velocity in m/s. The depths of 2086th, 2166th, 2888th, 3008th and 3072nd meters were selected, their acoustic impedance values were determined from the log.

Table 3.2: Depth, Time (TWT), Mud weight, pressure and acoustic impedance table.

Depth (m)	Time (ms)	Mud Weight (ppg)	Pressure (psi)	Acoustic Impedance (m/s * g/cc)
2086	1656	9.5	3381	7000
2166	1693	9.5	3510.7	7200
2888	2134	11	5420	6600
3008	2200	11	5645	6096
3072	2253	11	5765	6045

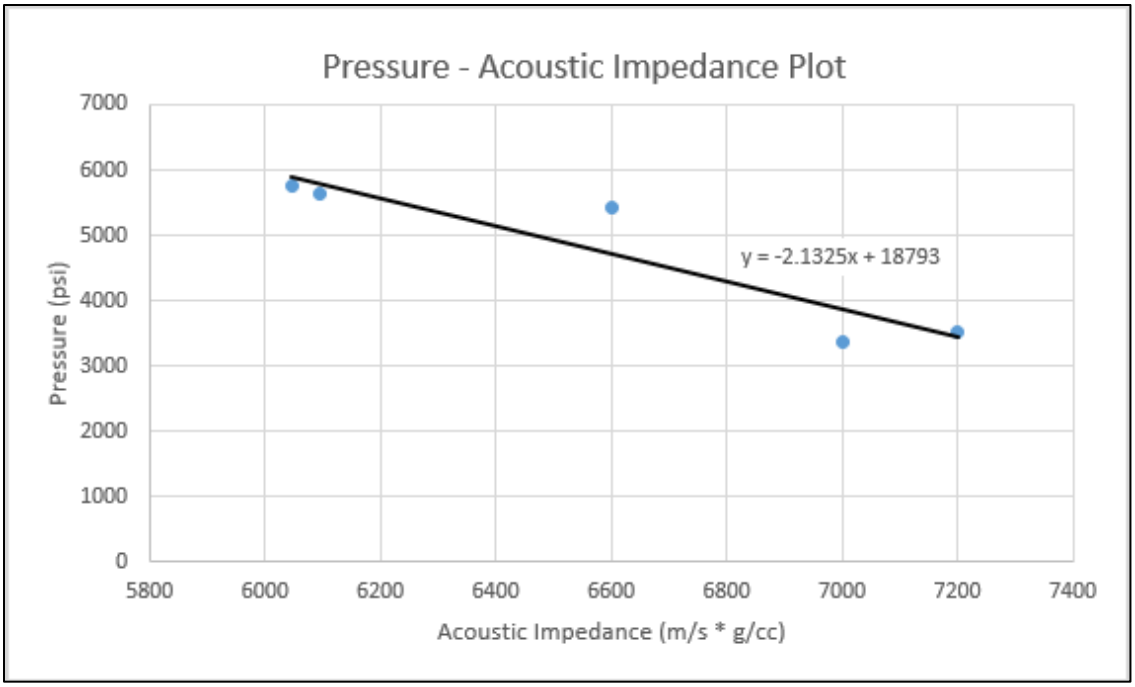

Figure 3.22: Pressure (psi) – Acoustic Impedance (m/s * g/cc) graphic by selected two depths in Table 3.2. Equation of the line is y=-2.1325x + 18793 that was obtained from excel.

We applied this equation to convert the acoustic impedance from inversion in Figure 3.21. In the equation, we used "x" an unknown value for acoustic impedance to obtain "y" an unknown value that corresponds to Pore Pressure in psi. This equation is only valid in the overpressure zone. That's why, the range of 100 ms above and 100 ms below of the overpressure zone horizon was taken into account.

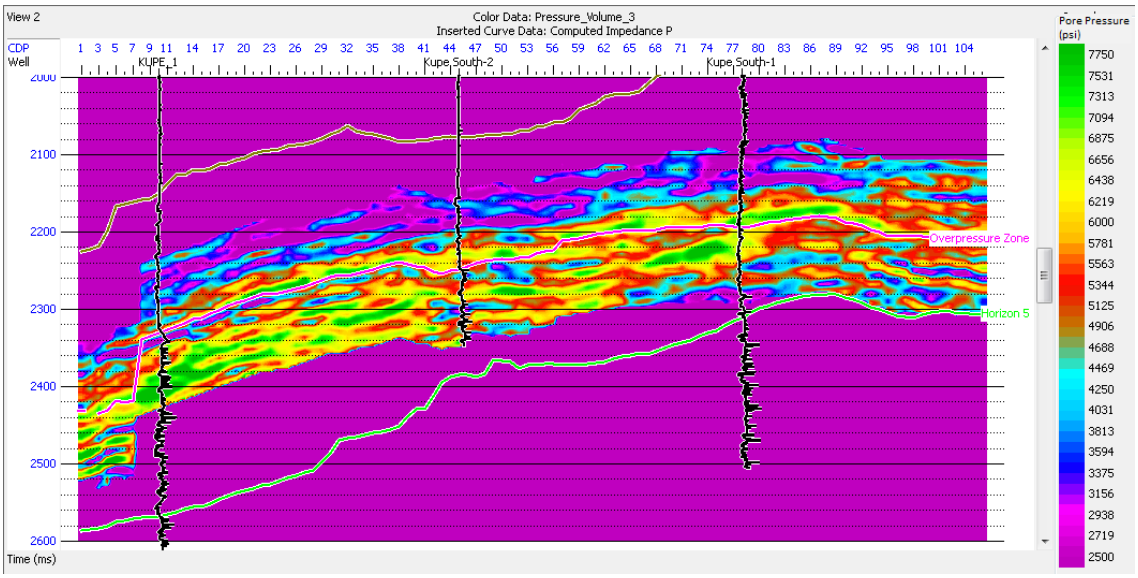

Figure 3.23: Pore pressure map that was obtained from the equation. Green and yellow colors show high pore pressure values. The other purple areas in large scale is uncalculated places.

4. Result & Discussion

As mentioned in previous chapters, overpressure is determined by using well responses, acoustic impedance and drilling event results, and by calibrating pressure to acoustic impedance from well logs and inversion. These results were summarized in this chapter for each well besides 3D maps given as final images.

Kupe South-1

- Mud weight increased from 5111 psi (10.65 ppg) to 5420 psi (11.0 ppg) at 2888 m in table 3.1.
- Trend lines were drawn on logs to see the differences better.
- Sonic log decreases with depth, but this trend changes in the Otaraoa formation shown in Figure 3.4. The density log also has a decreasing trend with depth. However, there is no change in the same formation. After passing this formation, all these logs continue their normal trend. These well log results follow the trend of mud weight and well log reports.
- In Figure 3.21, my seismic response to this overpressure with that acoustic impedance decrease in Otaraoa formation.

Kupe South-2

- Mud weight dramatically increase from 4136 psi (9.3 ppg) to 5445 psi (10.8 ppg) in 2955 m in anticipation of overpressure.
- The sonic log shows high values in the Otaraoa formation in Figure 3.5. The density log is not enough to determine overpressure.

- Acoustic impedance values are low in the Otaraoa formation in Figure 3.21. This result corresponds to log values and mud weight changes.

Kupe-1

- There is no well completion report of the Kupe-1 well. Therefore, we cannot get mud weight information.
- The sonic log starts increasing in the Otaraoa Formation in Figure 3.6. There is no density log in this formation.
- Acoustic impedance show low values under Otaraoa formation in Figure 3.21.

To see the overpressure zones on 3D map, volume and data slice maps are between 100 ms above and 100 ms below of overpressure zone horizon were created because that range covers low acoustic impedance areas in the Otaraoa Formation. The slice and volume map were set to show high pore pressure values in the time domain. These two maps show the overpressure zones in Kupe Field. We applied this calibration method by using only the Kupe South-1 well because it is the only well with complete data for determining both acoustic impedance and overpressure. This calibration is valid for the other wells and the whole field because their lithology in the Otaraoa formation is similar (see Figures 2.2, 2.3, and 2.4). We also correlated their sonic logs in the Otaraoa Formation, and these logs are also similar (Figure 4.3). According to these similarities, their pressure results are expected to be similar. It is also seen in the pressure-depth plot in Figure 4.4, overpressure zone is below 8000 ft (2400 m). Overpressure is below 56% of lithostatic pressure.

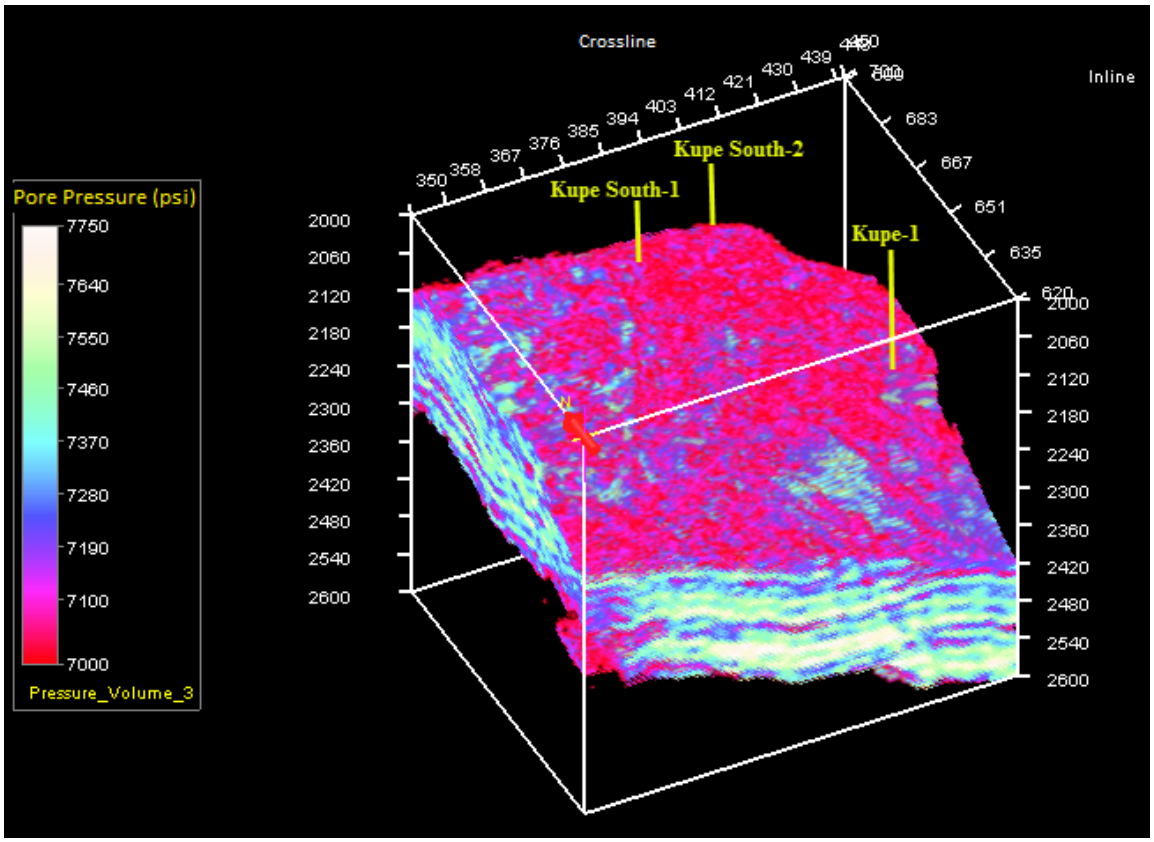

Figure 4.1: 3D volume map of the overpressure zone in time domain. These colors show the pore pressure values. Bright colors correspond to high pore pressure values, and dark colors correspond to low pore pressure values. Color scale was set to show pore pressure values higher than 7000 psi.

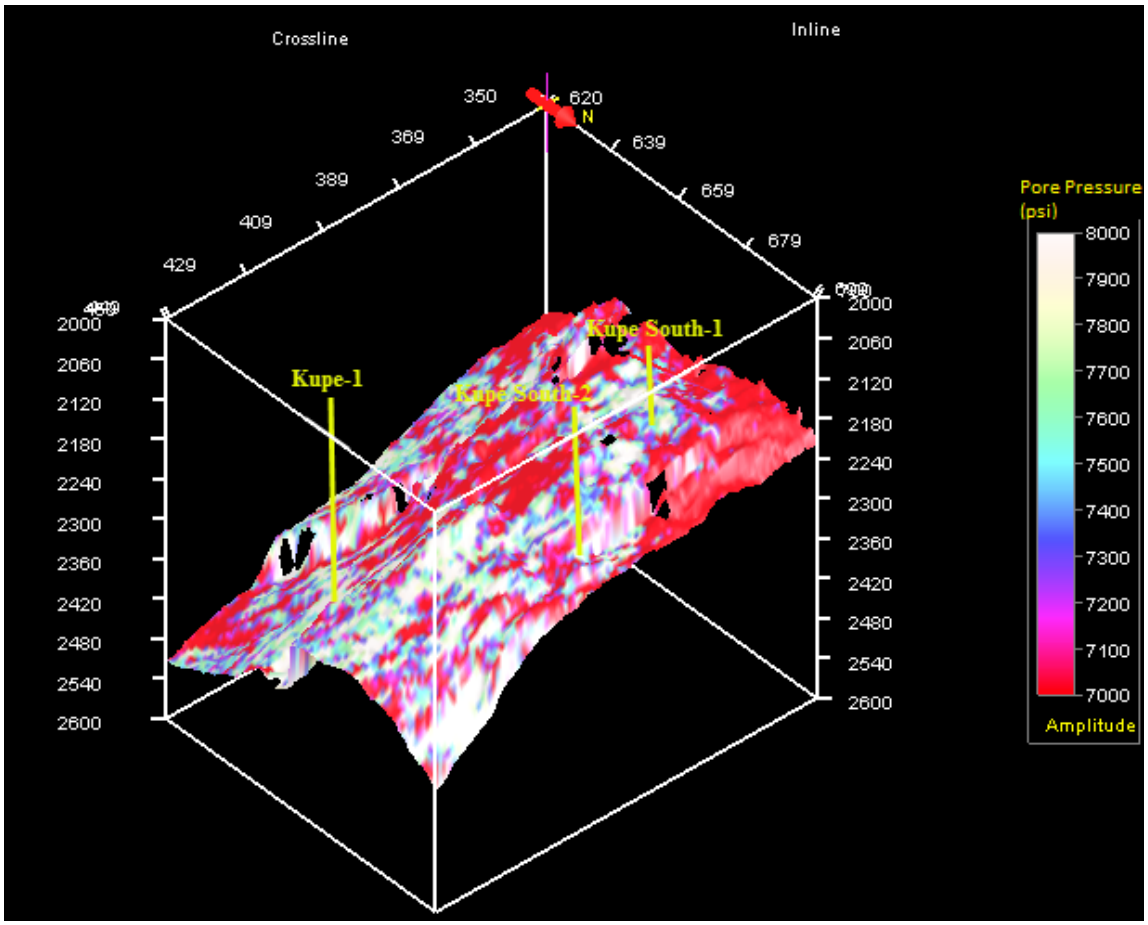

Figure 4.2: 3D map of slice that show maximum pore pressure values in time domain. Color scale was set to show pore pressure values higher than 7000 psi.

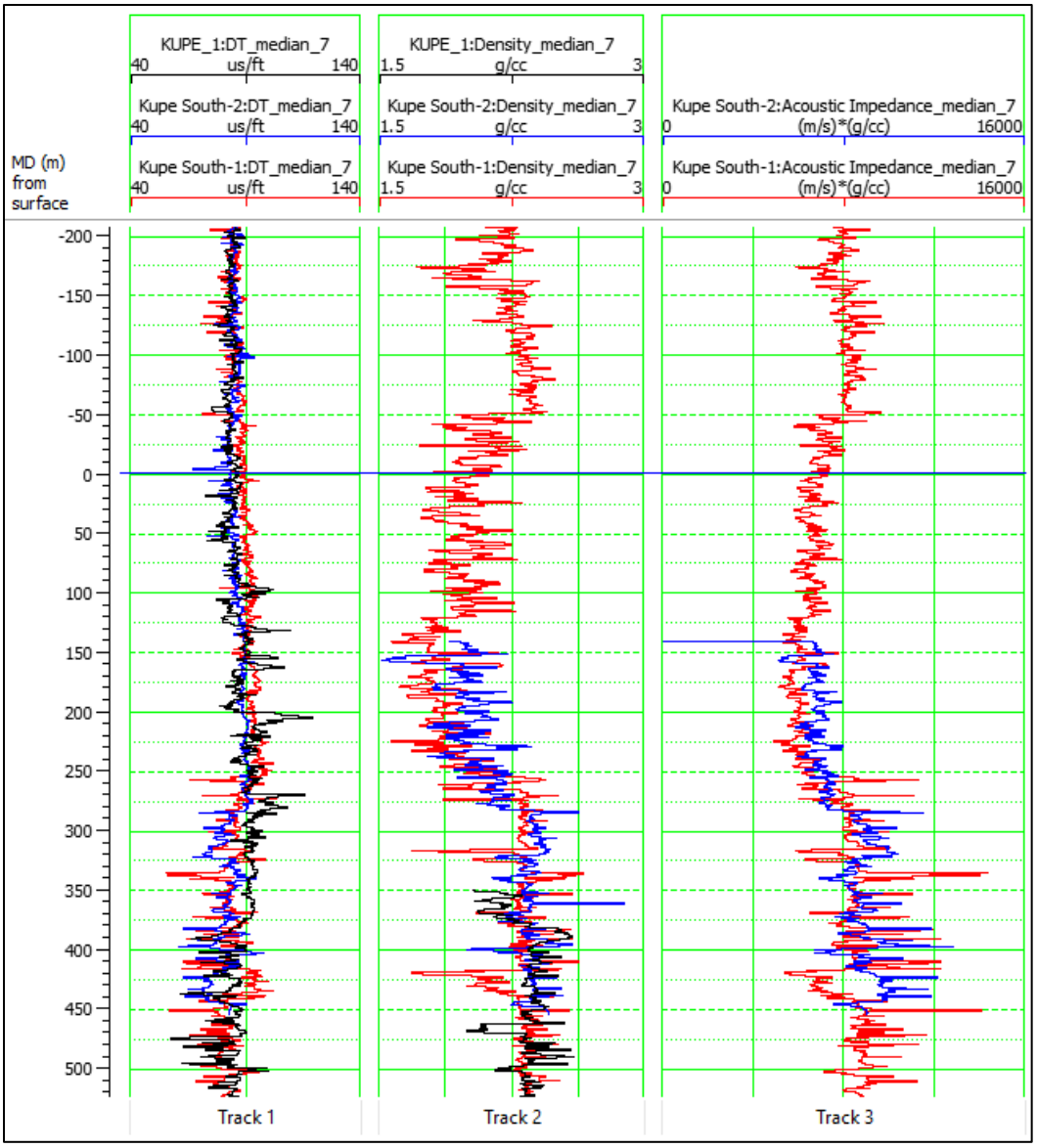

Figure 4.3: Correlation of sonic, density and acoustic impedance logs for three wells. Red curves show Kupe South-1 well logs (Sonic in µs/ft, density in g/cc and acoustic impedance in m/s * g/cc), blue curves show Kupe South-2 well logs (Sonic in us/ft, density in g/cc and acoustic impedance in m/s * g/cc), and black curves show Kupe-1 well logs (Sonic in µs/ft, density in g/cc). Track 1: Sonic logs; Track 2: Density logs; Track 3: Acoustic impedance logs. Blue horizontal line at 0 meter is the top of Otaraoa Formation for all wells. When we look at these correlations, curves for each well are similar so pressure for each well is expected to be similar.

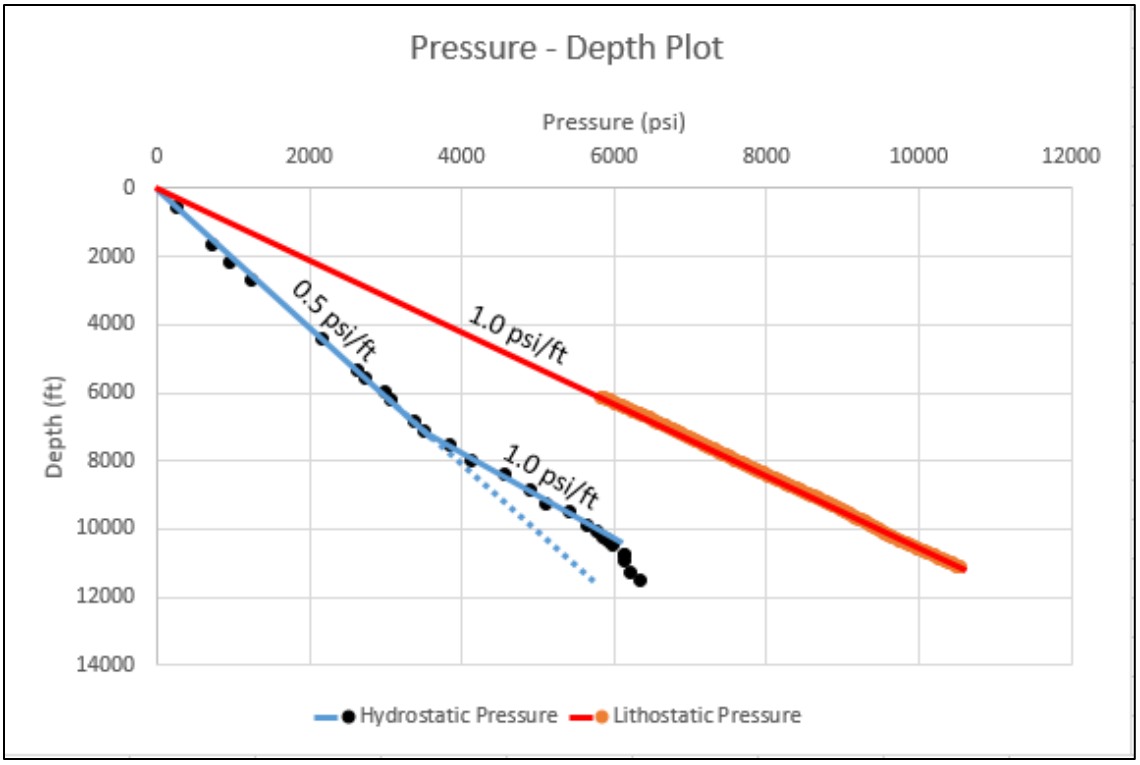

Figure 4.4: The black dots and the blue line are hydrostatic pressure based on mud weight of Kupe South-1 well. Orange dots are the lithostatic pressure values that were obtained from the equation of P=ρdg. P is pressure in Pa, ρ is average density of each 10 meters from the top of density log of Kupe South-1 well in kg/m^3, d is the thickness of each interval (10 meters) in m, and g is the acceleration due to gravity (9.8 m/s^2). The top of density log was determined as 2.2 g/cc. After calculation, pressure values were converted from Pa to psi, and depth values were converted from m to ft. Lithostatic pressure gradient was obtained 1.0 psi/ft.

5. Conclusion

The reason for overpressure in Kupe field is compaction disequilibrium which is a loading mechanism (Webster et al., 2010). To detect overpressure zones, seismic data, wireline logs such as sonic, density and acoustic impedance, and drilling events such as mud weight are analyzed. In this study, post-stack seismic data was inverted by using model-based inversion which is deterministic inversion method, to obtain acoustic impedance model. Low acoustic impedance indicates that there could be an overpressure zone. A sonic log decreases with depth, while a density log increases under normal conditions. However, these logs change their trends in an overpressure zone. Mud weight is another indicator of overpressure if mud weight suddenly increases.

Kupe South-2 well shows a great increase in mud weight in the Otaraoa formation. Kupe South-1 well's mud weight values also increase but slowly. The Kupe-1 well doesn't have mud weight report.

Kupe South-1 well affects the changing trend of well logs in the Otaraoa formation. When the density log decreases, the sonic log increases. The Kupe South-2 and Kupe-1 wells do not have enough well log information, such as density. Their sonic logs follow the rule of overpressure zone.

Overpressure in the Kupe field is seen in the Otaraoa formation. When we focus on this formation on the inversion map in Figure 3.21, it is clearly seen that all wells have very low acoustic impedance values under the Otaraoa Formation.

Pressure values which were obtained from mud weights were calibrated with the acoustic impedance log of Kupe South-1 well. The obtained equation from acoustic impedance –

pressure graphic was used to calibrate with acoustic impedance from inversion at an overpressure zone to get pore pressure map. In addition to this map, 3D volume and slice maps represent pore pressure values in the Otaraoa Formation. Green and yellow areas show the highest pore pressure values on the 3D maps.

Overall, we can clearly say that the Otaraoa Formation is an overpressure zone. The depths and locations of the overpressure zones are presented in 3D maps in detail.

6. References

Badri, M. A., Sayers, C. M., Awad, R., and Graziano, A., 2000, A feasibility study for pore-pressure prediction using seismic velocities in the offshore Nile Delta, Egypt. The Leading Edge, October, 1103-1108.

Barclay, F., Bruun, A., Rasmussen, K. B., Alfrado, J. C., Cooke, A., Cooke, D., Roberts, R., 2008, Seismic inversion: Reading between the lines: Oilfield Review, 20, no.1, p. 42-63

Bowers, G.L., 1995, Pore pressure estimation from velocity data: accounting for overpressure mechanisms besides undercompaction: SPE Drilling and Completion, 10, 89-95

CGG Australia Services Pty Ltd, 2004, Reprocessing Report for Kerry 3D Survey: Origin Energy Resources Limited - KS96 Kerry 3D Marine Project No: 502p1cz

Darby, D., R. Funnell, and V. Stagpoole, 2000, Overpressure, seal breaching and stress regimes in East Coast and Taranaki basins, New Zealand (abs.): AAPG International Conference and Exhibition, Bali, Indonesia, 1 p.

Donaldson, I. F., C. J. Way and J. A. Wellensiek, 1987, Kupe South-2 well completion report PPL 38116: Ministry of Economic Development Petroleum Report 1285

Dutta, C. N., 2002, Geopressure Prediction using seismic data: Current status and the road ahead. GEOPHYSICS, VOL. 67, NO. 6; P. 2012–2041, 34 FIGS., 4 TABLES,10.1190/1.1527101.

Eaton, B.A., 1972, Graphical method predicts geopressures worldwide: World Oil, 182, 51-56

Hubbert, M. K., and Rubey, W. W., 1959, Role of fluid pressures in mechanics of overthrust faulting: Geol. Soc. Am. Bull., 70, 115–166.

Lowry, D., 2006, Kapuni C sands regional pressure regime and implications for the Opito updip and Felix leads: Ministry of Economic Development Petroleum Report 3411

Matthews, E., and C. Lewis, 2001, Geophysical definition of Kapuni coastal facies of the western Taranaki Basin, New Zealand: Petroleum Exploration Society of Australia Eastern Australian Basins Symposium, p. 141-149.

Matthews, E.R., and D.J. Bennett, 1987, Kupe South-1 Well Completion Report PPL 38116

Mouchet, J.-C., Mitchell, A., 1989, Abnormal Pressures While Drilling. Editions TECHNIP, Paris.

Ramdhan, A.M., Goulty, N.R., and Hutasoit, L.M., 2011, The Challenge of Pore Pressure Prediction in Indonesia's Warm Neogene Basins, Proceedings of Indonesian Petroleum Association, 35th Annual Convention, IPA11-G-141

Shell BP Todd Oil Services Limited, 1976, Kupe-1 well completion report PR662

Shell Todd Oil Services Limited, 2002, Technical evaluation, licence PPL 38705: Ministry of Economic Development Petroleum Report 2709

Webster, M., O'Connor, S.A., Pindar, B. and Swarbrick, R.E., 2010, Overpressures in the Taranaki Basin: Distribution, Causes and Implications for Exploration. AAPG BULLETIN V.95, NO. 3 (MARCH, 2011), pp. 339-370

Webster, M., and S. Adams, 1996, Geopressures and hydrocarbon generation and migration onshore Taranaki: Petroleum Exploration in New Zealand News, Ministry of Commerce, 47 p. 13-22.

Yosandian, H. H., Irawan, H., Ulum, B. W. A., Tribuana, I. Y., and Embara, P., 2014, Overpressure characteristic in the Langkat Field, North Sumatra Basin, Indonesia. 2014 3rd International Conference on Geological and Environmental Sciences, IPCBEE vol. 73 (2014) © (2014) IACSIT Press, Singapore, DOI: 10.7763/IPCBEE. 2014 V73. 9 p. 40-44

Zhang, J., 2013, Effective stress, porosity, velocity and abnormal pore pressure prediction accounting for compaction disequilibrium and unloading. Marine and Petroleum Geology 45 (2013) p. 2-11

7. Copyright Permission

Figure 1.1, 3.7 and 3.8 Google Image Copyright Permission

Thanks for considering Google Maps, Google Earth and Street View for your project! These guidelines are for non-commercial use except for the limited use cases described below; if you want to use Google Maps, Google Earth, or Street View for other commercial purposes, please contact the Google Cloud Customer Team. “Commercial purposes” means “use for sale or revenue-generating purposes”.

We created this page to clarify questions we’ve received from users over the years regarding uses of our mapping tools in everything from marketing and promotional materials, films, television programs, books, academic journals, and much more.

Generally speaking, as long as you’re following our Terms of Service and you’re attributing properly, we’re cool with your using our maps and imagery; in fact, we love seeing all of the creative applications of Google Maps, Google Earth and Street View! But we know you’re looking for more specifics to ensure you’re using our maps and imagery correctly.

As you dive into the information below, we suggest starting with the general guidelines at the top, as these will apply to all projects. Then feel free to click directly to the section that applies to you

https://www.google.com/permissions/geoguidelines.html#generalguidelines

Figures 2.2, 2.3, 2.4, 3.1, 3.7 and 3.8 GNS Science Copyright Permission

Hi Timucin

Yes you have our permission to use PBE maps, lithologies and seismic workflow in your thesis. Please credit GNS Science and the Petroleum Basin Explorer website. Our full terms and conditions can be read here
https://data.gns.cri.nz/dataportal/terms.jsp

Cheers,
Andrew

Andrew Boyes | Technical Support Specialist
GNS Science | Te Pū Ao
1 Fairway Drive, Avalon 5010, PO Box 30368, Lower Hutt 5040, New Zealand
Ph 04 570 4287 | Mob 027 335 3150 |
https://www.gns.cri.nz/ | Email: a.boyes@gns.cri.nz

Figure 2.1 The responses of well logs to loading mechanism Copyright Permission

Dear Timucin,

Neil forwarded me your email regarding using our figure in "The Challenge of Pore Pressure Prediction in Indonesia's Warm Neogene Basins (2011)". It is public domain already, so actually you can freely use the figure without our permission. However, thanks very much for asking that - it is really appreciated. All the very best for your thesis.

Best regards,

Agus